AN INTERFEROMETRIC METHOD FOR THE DETERMINATION OF BINARY DIFFUSION COEFFICIENTS

A Thesis

Presented to

The Faculty of the Division of Graduate

Studies and Research

By

Robert Lee Somers

In Partial Fulfillment

of the Requirements for the Degree

Master of Science in Mechanical Engineering

Georgia Institute of Technology

March, 1974

AN INTERFEROMETRIC METHOD FOR THE DETERMINATION

OF BINARY DIFFUSION COEFFICIENTS

Approved:

/

William Z. Black, Chairman

Charles W. Gorton

Henderson C. Ward

Date approved by Chairman: 2/27/74

ACKNOWLEDGEMENTS

I wish to express my gratitude to my advisor, Dr. William Z. Black, for his guidance of my research and aid in the preparation of this thesis. I also thank the members of my reading committee, Dr. C. W. Gorton and Dr. H. C. Ward for their advise and corrections. Thanks also go to Dr. Chuck Carr for his help during the testing and generous sharing of his interferometric experience.

Recognition must go to the technicians of the School of Mechanical Engineering for their contributions. Mr. H. J. Carr was the machinist who built the test cell, Mr. J. Doyal and Mr. L. Cavelli helped with their experience, and Mr. T. E. Clopton provided electronic expertise and a helping hand in setting up the temperature measurement and recording equipment.

Finally, the financial assistance provided by the United States Government, the Selby Foundation, and especially the author's family was greatly appreciated.

TABLE OF CONTENTS

LIST OF TABLES

LIST OF ILLUSTRATIONS

NOMENCLATURE

Symbol	Definition	Units
c	Molar density	gm-moles/cm^3
D_{AB}	Mass diffusivity	cm^2/sec
E	Coordinate similarity parameter	Dimensionless
g	Distance between first Wollaston prism and spherical mirror	Centimeters
K	Constant	Variable
L	Length of light path through test cell	Centimeters
m	Number of fringe shifts	Dimensionless
M	Molecular weight	gm/gm-mole
n	Index of refraction	Dimensionless
n_{DB}	Index of refraction of dry air	Dimensionless
n_e	Extraordinary index of refraction of birefringent material	Dimensionless
n_o	Ordinary index of refraction of birefringent material	Dimensionless
N	Molar refractivity	ml/gm-mole
$\bar{N}$	Molar flux	gm-mole/cm^2sec
P	Pressure	atm, mm of Hg
P_r	Reference pressure = 760 mm Hg used in correcting index of refraction	mm of Hg
P_v	Vapor pressure of diffusing substance	mm of Hg
P_{tr}	Test result parameter	1/sec.
Q	Molar average velocity	Dimensionless

Symbol	Definition	Units
r	Fringe shift correction factor	Dimensionless
R	Molar rate of production	gm-mole/cm^3sec
$\bar{R}$	Universal gas constant	atm-ml/gm-mole°K
t	Time	Seconds
T	Temperature	°K, °C
T_r	Reference temperature = 288°K used in correcting index of refraction	°K
x	Mole fraction	Dimensionless
X	Concentration similarity parameter	Dimensionless
z	Coordinate perpendicular to evaporating surface	Centimeters
Δz	Separation distance	Centimeters
λ	Wavelength	Angstroms
ρ	Density	gm/cm^3
θ	Wollaston prism angle	Radians
$\Delta\phi$	Phase difference introduced in test section	Centimeters

Subscripts

a	Quantity at time t_a
A	Property of diffusing substance
b	Quantity at time t_b
B	Property of air
cr	Corrected
P	Property at pressure P
t	Quantity at time t
T	Property at temperature T

Subscripts

wv	Property of water vapor in the air
z	Quantity in direction z
z_1	Quantity at distance z_1 from liquid-gas interface
z_2	Quantity at distance z_2 from liquid-gas interface
0	Quantity at interface
1, 2, 3	Numbers of constants

SUMMARY

This thesis describes the application of an interferometer capable of determining concentration gradients to the measurement of binary diffusion coefficients. The objectives of the study were to develop a technique adaptable to the differential interferometer for the determination of the diffusivity of volatile liquids; assess the method for practicality and accuracy; and apply the technique to the evaluation of the diffusivities of substances previously unreported.

The method used a differential interferometer with three Wollaston Prisms, a high-speed camera, and a timing device to record the change in concentration gradient with time during the diffusion process. A test cell was constructed that modeled the transient one-dimensional evaporation of volatile liquid into stagnant air. The equations describing this process were adapted to a relative time solution and modified to make use of interferometrically generated data.

Tests were conducted on eleven of the seventeen test substances selected for potential investigation. Data are presented for five substances whose diffusivities are available in literature. Differences from established values varied from 3.9 percent low to 23.5 percent low. All tests produced diffusivity values below the accepted norm. Data are also presented on three previously unreported substances. The remaining nine substances selected for possible study are unreported due to incompatibility with the test system.

The main cause of error in the reported diffusivities was poor modeling of the theoretical initial condition by the test cell. Premature diffusion, which occurred in most tests, was dependent on the volatility of the substance being tested. The conclusion was reached that, while the interferometer was adaptable to diffusion study and capable of producing diffusivity data in a relatively short time, the method developed in this investigation was less accurate than other techniques. The additional conclusion was reached that the number of substances suitable for interferometric diffusivity determination are relatively limited.

CHAPTER I

INTRODUCTION AND BACKGROUND

The ability of the interferometer to provide data on concentration and temperature distributions makes it an extremely useful tool in the study of heat and mass transfer. The change in temperature and/or concentration distributions produces a change in the pattern of index of refraction which may be detected through the use of an interferometer. The device is also useful since it has little or no effect on the process under study and it also is suitable for the consideration of rapidly changing transient phenomena when coupled with a high-speed camera system.

The use of optical methods based on interference patterns to study diffusion is not a recent development. Many investigators have applied numerous interesting techniques. The great majority have been applied to diffusion in liquids, as the following examples indicate.

Kegeles and Gostling [35] presented in 1947 the theory for a fringe system that would be formed by passing the light from a slit through a diffusing boundary. This was a redevelopment of the much older Gouy interference method of 1880. Longsworth [36] and Ogston [45] made use of optical devices called Gouy diffusiometers to experimentally verify the theoretical predictions of Kegeles and Gostling. Coulson and co-workers [17] applied similar techniques to find the diffusion constant for a dilute solution-solvent system. In 1950

Longsworth [37] presented results obtained using flowing junction cells and the Gouy diffusiometer applied to liquid diffusion.

Philpot and Cook [48] modified a Rayleigh interference refractometer in 1948 to use in liquid diffusion study. A two cell technique with a focusing lens was utilized in which the results obtained represented local difference in index of refraction. Nicolas and Calvet [43] also made use of the Rayleigh type interferometer and a two cell method to study liquid diffusion and sedimentation.

Svensson [60, 61, 62, 63, 64, 65, 66] published numerous articles between 1949 and 1952 concerning the development of a new interferometric technique in liquid diffusion. Based upon the earlier work of Philpot and Cook, a Rayleigh interferometer was modified to measure both refractive index and its gradient by changing the arrangement of the slits. Svensson demonstrated the use of the system by measuring diffusion in a sugar/water system. Further development of the optics involved replacing the single slit of the Rayleigh interferometer with a device that produced fringes of the higher intensity needed in the studies.

Robinson [53] developed an interferometric technique to study diffusion in polymers and with Crank [18] applied the method to the study of the action of five penetrants. The Jamin type interferometer was adapted in 1952 by Antweiler [2] to study sedimentation, electrophoresis and diffusion constants. Saini and Moraglio [56] used the apparatus developed by Anteweiler to study the diffusion of a one percent sucrose solution in water.

The use of the Wollaston Prism in diffusion studies was introduced by Weinstein [75] in 1953. Use was made of a single prism to

split a ray from a monochromatic light source. The split ray was passed through a twin cell and back through the prism. Fringes were produced on an image of the cell that could be interpreted in terms of both the index of refraction and its gradient.

The use of birefringence interference produced by Savart plates was first used by Ingelstam [32] in 1955. The technique was applied to the diffusion of amino-acetic acid (glycine) in water. Bryngdahl [9, 10, 11, 12, 13] also made use of Savart plates in work on liquids in which diffusion and boundary formation were studies and the deviation from ideal conditions was investigated. Later, the limitations of the Savart type interferometer were discussed by Porsch and Kubin [49] who, in 1968, proposed a more general method than that of Bryngdahl.

In the 1960's other new methods of investigation were applied to liquid diffusion by Caldwell, Hall, and Babb [14] who first used the Mach-Zehnder interferometer and Hariharan and Sen [29] who modified a three beam instrument to find concentrations of a solution along a vertical axis. Hook, Davis, and Kotin [31] used a computer to evaluate Rayleigh fringe displacements. A method that made use of Moiré interference patterns was demonstrated by Nishijima and Oster [44] in 1964. Inoue, Osugi, and Inoue [33] developed new diffusion cells for use with a Schlieren knife edge method in liquid state studies.

Further developmental work in the 1960's was carried out by Thomas and Nicholli [67] who used Savart plate interferences and a flowing junction cell to study a sucrose-water problem. A double Savart plate interferometer was utilized by Haluska and Colver [28] to determine the diffusion coefficient of toluene in methyl-cyclohexane.

Paul [46] in 1967 described a very simple interference technique using partially reflecting microscope slides in a wedge with a very small angle. The device was used to determine concentration profiles in polymer-solvent diffusion. Duda, Sigelko, and Vreitas [21] also used partially reflecting plates to measure the diffusion coefficient in a concentration dependent sucrose-water system. Results of the measurements pointed out the determinations using the simple wedge device are subject to significant errors unless great care is exercised.

Another variation in liquid diffusion study was introduced in 1968 by Travincek and Fan [69]. A laser light source was combined with a Fabry-Perot interferometer to measure the diffusion coefficient of benzene in cyclohexane. A laser was also used in the diffusion layer studies of Watkins and Tvarusko [73] using a Lloyd mirror interferometer. An interesting development was the use of an array of n-p-n silicon photo cells to detect interference fringe movement.

More recently the interferometer has been applied to the thermal diffusion problem in liquids. In 1962 Chanu, Mousselin and Parra [16] described an optical method for thermal diffusion measurement. Bierlein [4] applied the principles of Gouy interference to binary liquid systems undergoing thermal diffusion. The Soret effect was measured in a cadmium sulfate water system by Wallin [71] in 1969. In this study use was made of a modified Savart interferometer and a double exposure photographic technique.

While numerous examples of the interferometric study of diffusion in the liquid state exist (as previously listed), cases involving evaporation or gas-gas diffusion are relatively rare. One gas-gas

diffusivity determination by interferometric means found in the literature was reported in 1951 by Boyd, Stein, Steingrimsson and Rumpel [8]. This reference describes a method for determining the diffusion coefficients in gaseous systems using a Loschmidt type cell. Using a Mach-Zehnder interferometer, the diffusivities of several gases in either hydrogen or nitrogen were measured.

In 1960 Ross and El-Wakil [54] presented a two-wavelength technique for the study of fuel vaporization. The use of the two wavelength method allows the separation of the temperature and concentration gradients detected in the fringe displacements produced by a modified Mach-Zehnder interferometer. A similar interferometer was used in 1964 by El-Wakil and Jaeck [22] in a two-wavelength study of the evaporation of n-hexane from a cylinder in cross airflow. The Mach-Zehnder system was used again in 1966 by El-Wakil with Meyers and Schilling [23] to study the concentration profiles in the steady state evaporation of a volatile liquid from a vertical plate in a heated airstream. Only one wavelength was used in this study since the assumption was made that the normalized temperature and concentration profiles were similar. Sadovnikov, Smol'skiy and Shchitnikov [55] also made use of a two-wavelength system in their determinations of simultaneous heat and mass transfer in a volatile fluid diffusion into air.

The evaporation of water has been investigated using the interferometer in two studies. Adams and Meier [1] used a Mach-Zehnder interferometer and a gas laser light source to observe the density gradients near a water-air interface. This work involved the evaporation of both heated and room temperature distilled water and it provided observation

of the changes in the thermal layer and temperature gradient in the region near the interface. Prasad, Chen and Beard [50] also have interferometrically studied the temperature and concentrations near a water-air interface. The purpose of the Prasad study was to devise an alternative to the two-wavelength technique for simultaneous heat and mass transfer study in which difficulties arise due to the insufficient independency of the equations.

Grob [26, 27] in a study similar to the work of this thesis investigated the diffusion of volatile liquids into air using a Mach-Zehnder interferometer. The method developed involved a relative time-relative position technique for the determination of diffusivity that eliminated the need of knowing the total mass flux from the evaporating surface.

Many of the interferometric methods used for studying diffusion phenomena listed in the literature review have been motivated by a desire to shorten the time required for diffusivity measurements. The methods proposed for diffusivity determinations fall mainly into three general categories. Two of the three techniques may be adapted for use with an interferometer. The Loschmidt [38] method is a transient, one-dimensional process using two equal volume chambers filled with different gases that are initially separated. The study of the interchange of the gases in the chambers after removal of the barrier between them can result in determination of the diffusivity. This method is limited to gases and is suitable for use with an interferometer.

A second method follows the work of Stephan [58] and consists of the steady state, one-dimensional evaporation of a liquid vapor into a

stagnant gas. The diffusion occurs in a long tube. The concentration of the diffusing gas must be fixed at the tube exit. This method is not adaptable to interferometric means but is still useful since gradient information is not necessary for diffusivity measurement.

The Arnold [3] technique is the most recently developed of the three major methods and involves the evaporation of a volatile liquid into a stagnant film of gas. It is a transient one-dimensional technique requiring initial separation of the components as in the Loschmidt method. It is similar to the Stephan method in that it also requires vapor pressure data.

A differential interferometer of the three Wollaston Prism type was available in the Georgia Institute of Technology School of Mechanical Engineering and had not previously been utilized in diffusion studies. The ability of this device to directly produce data on the gradient of index of refraction and in turn concentration gradient made its application to diffusivity studies natural. The investigation of liquid-liquid diffusion was avoided due to the great amount of interferometric study already done on liquid systems and the evaluation of the evaporation of volatile liquids was undertaken. A modified Arnold technique was used in conjunction with a diffusion cell-differential interferometer-high-speed camera system to determine diffusities. This work used an adaptation of Grob's relative time solution applied to the differential interferometer. Since the interferometer used produced information about gradient in index of refraction, a significant simplification in Grob's method could be realized due to the elimination of the relative position slope calculation.

CHAPTER II

THEORETICAL DEVELOPMENT

The diffusion process under consideration consists of the unsteady evaporation of a species A into a second, stagnant species B. The theory which follows is limited by the following assumptions:

1. Species A and B form an ideal gas mixture.

2. The temperature and total pressure are uniform throughout the system. Thus, no thermal or pressure diffusion occur and the molar density of the mixture, c, and the diffusivity, D_{AB}, are constants.

3. Species B is insoluble in liquid A.

4. The diffusion is one-dimensional and occurs in an infinitely high channel.

5. No chemical reactions occur.

6. Equilibrium exists at the liquid-gas interface. The diffusion system is shown schematically in Figure 1.

A mass balance applied to a differential element located an arbitrary distance, z, above the liquid interface yields the continuity equation for both species [5]

$$\frac{\partial c_A}{\partial t} + (\nabla \cdot \bar{N}_A) = R_A \qquad \text{(II-1A)}$$

$$\frac{\partial c_B}{\partial t} + (\nabla \cdot \bar{N}_B) = R_B \qquad \text{(II-1B)}$$

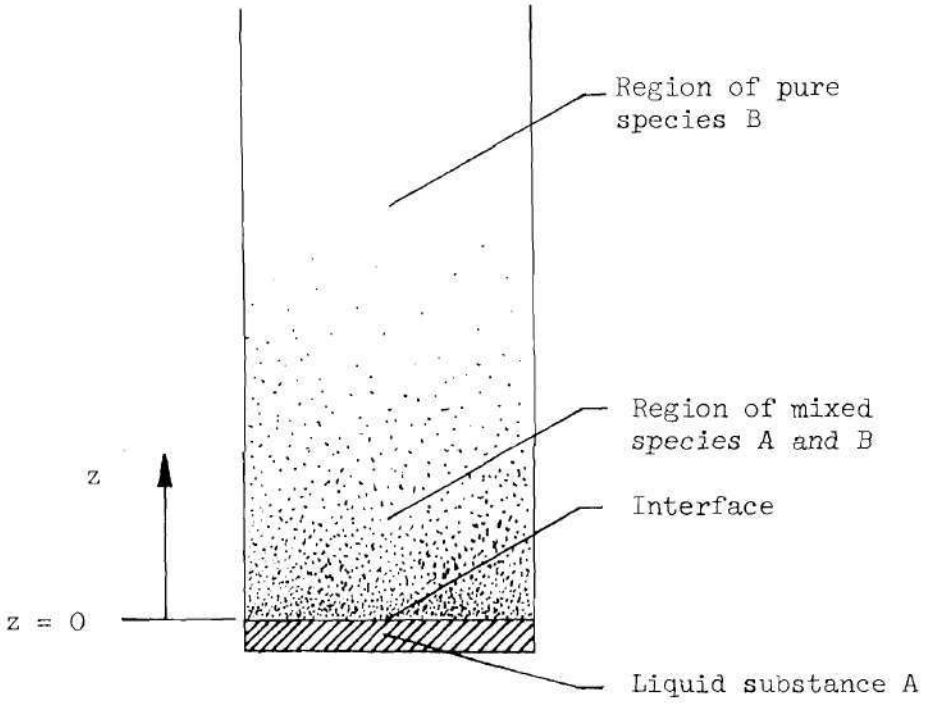

Figure 1. Schematic Drawing of Diffusion System

Applying the assumptions of one dimensionality and the absence of chemical reactions simplifies equations (II-1) to

$$\frac{\partial c_A}{\partial t} = - \frac{\partial \bar{N}_{Az}}{\partial z} \qquad \text{(II-2A)}$$

$$\frac{\partial c_B}{\partial z} = - \frac{\partial \bar{N}_{Bz}}{\partial z} \qquad \text{(II-2B)}$$

Adding gives

$$\frac{\partial c_A}{\partial t} + \frac{\partial c_B}{\partial t} = \frac{\partial}{\partial t} (c_A + c_B) = - \frac{\partial \bar{N}_{Az}}{\partial z} - \frac{\partial \bar{N}_{Bz}}{\partial z} \qquad \text{(II-3)}$$

Since the mixture of species A and B has been assumed to be a perfect gas with uniform temperature and total pressure

$$c_A + c_B = c = \text{constant}$$

Thus

$$\frac{\partial(c_A + c_B)}{\partial t} = \frac{\partial c}{\partial t} = 0 = - \frac{\partial}{\partial z} (\bar{N}_{Az} - \bar{N}_{Bz}) \qquad \text{(II-4)}$$

Since the quantity $(N_{Az} + N_{Bz})$ has been shown to be independent of z, it must be a function of time only.

Fick's First Law may be written in the form

$$\bar{N}_A = x_A(\bar{N}_A + \bar{N}_B) - cD_{AB} \nabla x_A \qquad \text{(II-5)}$$

Since the vapor of species B is assumed insoluble in liquid A, the flux of species B must be zero at the liquid-gas interface. Rewriting Fick's Law at the interface (z = 0) gives

$$\bar{N}_{AO} = x_{AO}(\bar{N}_{AO} + 0) - cD_{AB} \nabla x_A \Big|_{z = 0} \qquad \text{(II-6)}$$

By rearranging and applying one-dimensionality

$$\bar{N}_{AO} = - \frac{cD_{AB}}{1-x_{AO}} \frac{\partial x_A}{\partial z} \Big|_{z = 0} \qquad \text{(II-7)}$$

Since the sum of the molar fluxes has been shown to be independent of z by Equation (II-4), the flux at the interface, $\overline{N}_{AO}$, must be equal to the total flux at any z. Thus

$$\overline{N}_{Az} + \overline{N}_{Bz} = \frac{-cD_{AB}}{1-x_{AO}} \frac{\partial x_A}{\partial z} \Big|_{z = 0} \qquad \text{(II-8)}$$

Substituting Equation (II-8) into Fick's Law (II-5) and applying the one-dimensional assumption again gives

$$\overline{N}_{Az} = x_A \left[\frac{-cD_{AB}}{1-x_{AO}} \frac{\partial x_A}{\partial z} \Big|_{z = 0} \right] - cD_{AB} \frac{\partial x_A}{\partial z} \qquad \text{(II-9)}$$

Equations (II-9) and (II-2A) can now be combined to produce

$$\frac{1}{c} \frac{\partial c_A}{\partial t} = \frac{\partial (c_A/c)}{\partial t} = \frac{\partial x_A}{\partial t} = D_{AB} \frac{\partial^2 x_A}{\partial z^2} +$$

$$\frac{D_{AB}}{1-x_{AO}} \frac{\partial x_A}{\partial z} \Big|_{z = 0} \frac{\partial x_A}{\partial z} \qquad \text{(II-10)}$$

where D_{AB} has been assumed to be a constant. The equilibrium mole fraction, x_{AO}, which appears in Equation (II-10) is equal to the ratio of the vapor pressure of substance A to the total pressure. This is a valid equality for all cases except those involving extremely high evaporation rates [24, 70].

The initial and boundary conditions to be applied to Equation (II-10) are

$$\text{For } t = 0 \; ; \quad x_A = 0 \quad \text{for } z > 0 \tag{II-11A}$$

$$\text{For } z = 0 \; ; \quad x_A = x_{AO} \quad \text{for } t > 0 \tag{II-11B}$$

$$\text{For } z = \infty \; ; \quad x_A = 0 \quad \text{for } t \geq 0 \tag{II-11C}$$

Equation (II-10) and the above conditions describe the transient, one-dimensional, diffusion process under consideration.

The solution of this system, given by Equation (II-21), is patterned after the work of Arnold [3]. The solution is obtained by defining the following two similarity parameters

$$X = \frac{x_A}{x_{AO}} \tag{II-12}$$

and

$$E = \frac{z}{\sqrt{4D_{AB}t}} \tag{II-13}$$

where X is a dimensionless concentration and E is a dimensionless coordinate perpendicular to the evaporating surface of species A. Assuming that X is a function of only E, for any x_{AO} Equation (II-10) becomes

$$\frac{d^2X}{dE^2} + 2(E - Q)\frac{dX}{dE} = 0 \tag{II-14}$$

where

$$Q = -\frac{1}{2}\frac{x_{AO}}{1-x_{AO}}\frac{dX}{dE}\Big|_{E=0} \neq f(E) \qquad \text{(II-15)}$$

which represents a dimensionless molar velocity. The transformed boundary conditions are

$$\text{For } E = 0 \; ; \quad X = 1 \qquad \text{(II-16A)}$$

$$\text{For } E = \infty \; ; \quad X = 0 \qquad \text{(II-16B)}$$

The transformed system of Equations (II-14) and (II-16) may be solved by setting

$$X' = \frac{dX}{dE} \qquad \text{(II-17)}$$

Equation (II-14) now becomes

$$\frac{dX'}{dE} + 2(E - Q)\, X' = 0 \qquad \text{(II-18)}$$

Separating the variables and integrating gives

$$K_1 \frac{dX}{dE} = \exp[-(E - Q)^2] \qquad \text{(II-19)}$$

Separating and integrating again yields

$$K_1 \frac{dX}{dE} = \frac{\sqrt{\pi}}{2} \operatorname{erf}(E - Q) + K_2 \qquad \text{(II-20)}$$

Application of the boundary conditions to Equations (II-19) and (II-20) gives the solution of Equation (II-14) as

$$X = \frac{1 - \operatorname{erf}(E - Q)}{1 + \operatorname{erf} Q} \qquad \text{(II-21)}$$

where the constants of integration are

$$K_1 = \frac{-\sqrt{\pi}}{2} [1 + \operatorname{erf} Q] \qquad \text{(II-22)}$$

$$K_2 = \frac{-\sqrt{\pi}}{2} \qquad \text{(II-23)}$$

The portion of Arnold's solution required for the determination of D_{AB} results from the combination of Equations (II-22) and (II-19) which yields

$$\frac{dX}{dE} = \frac{\exp[-(E - Q)^2]}{\frac{-\sqrt{\pi}}{2} [1 + \operatorname{erf} Q]} \qquad \text{(II-24)}$$

This expression will be used in the relative time manipulation of the similarity parameter E that results in an expression for D_{AB} in terms of measurable quantities. Also obtained from the solution is a new expression for Q

$$x_{AO} = \frac{P_A}{P}\Big|_{z = 0} = \frac{1}{1 + \dfrac{1}{(1 + \operatorname{erf} Q) \exp[Q^2] \, Q \sqrt{\pi}}} \qquad \text{(II-25)}$$

which is the result of combining Equations (II-15) and (II-24).

Recall the definition of the dimensionless coordinate E

$$E = \frac{z}{\sqrt{4D_{AB}t}} \tag{II-13}$$

For given times t_a and t_b the derivatives of E are

$$\frac{\partial E}{\partial z}\Big|_{t_a} = \frac{1}{\sqrt{4D_{AB}t_a}} \tag{II-26A}$$

$$\frac{\partial E}{\partial z}\Big|_{t_b} = \frac{1}{\sqrt{4D_{AB}t_b}} \tag{II-26B}$$

Solving Equations (II-26) for time gives

$$t_a = \frac{1}{4D_{AB}}\left(1/\frac{\partial E}{\partial z}\right)_a^2 \tag{II-27A}$$

$$t_b = \frac{1}{4D_{AB}}\left(1/\frac{\partial E}{\partial z}\right)_b^2 \tag{II-27B}$$

Substracting and solving for D_{AB} gives

$$D_{AB} = \frac{1}{4(t_b - t_a)}\left[\left(1/\frac{\partial E}{\partial z}\right)_b^2 - \left(1/\frac{\partial E}{\partial z}\right)_a^2\right] \tag{II-28}$$

which is valid at any distance above the interface. For continuous derivatives

$$\frac{\partial X}{\partial z} = \frac{dX}{dE}\frac{\partial E}{\partial z} \tag{II-29}$$

The information obtained from the solution of Equation (II-14) is now used to convert from the similarity parameter E to the vertical coordinate z by substituting Equation (II-24) into (II-29). After rearrangement this procedure yields

$$\left(1/\frac{\partial E}{\partial z} \right) = \frac{-2\ \exp[-(E - Q)^2]}{\sqrt{\pi}\ (1 + \text{erf}\ Q)\ (\partial X/\partial z)} \tag{II-30}$$

Substitution into Equation (II-28) gives

$$D_{AB} = \frac{1}{t_b - t_a}\left[\frac{1}{\sqrt{\pi}\ (1 + \text{erf}\ Q)} \right]^2 \left[\left(\frac{1}{\exp[(E-Q)^2]\ \frac{\partial X}{\partial z}} \right)_b^2 - \left(\frac{1}{\exp[(E-Q)^2]\ \frac{\partial X}{\partial z}} \right)_a^2 \right] \tag{II-31}$$

From the definition of X (II-12) it follows that

$$\frac{\partial X}{\partial z} = \frac{1}{x_{AO}}\frac{\partial x_A}{\partial z} \tag{II-32}$$

Thus

$$D_{AB} = \frac{x_{AO}^2}{(t_b - t_a)\pi(1 + \text{erf}\ Q)^2}\left[\left(\frac{1}{\exp[(E-Q)^2]\ \frac{\partial x_A}{\partial z}} \right)_b^2 \right.$$

$$- \left(\frac{1}{\exp[(E-Q)^2] \frac{\partial x_A}{\partial z}} \right)_a^2] \qquad \text{(II-33)}$$

Since the proposed method for measurement of D_{AB} involves an optical technique, Equation (II-33) for diffusivity must be expressed in terms of interferometric parameters. This deriviation follows in the analysis below.

The index of refraction for a mixture of two gases, A and B, is

$$n = n_A + n_B - 1 \qquad \text{(II-34)}$$

The Lorenz-Lorentz Equation for molar refractivity, N is

$$N = \frac{n^2 - 1}{n^2 + 2} \frac{M}{\rho} \qquad \text{(II-35)}$$

For gases whose index of refraction is very close to 1.0, this equation may be reduced to

$$n = \frac{3}{2} \frac{\rho N}{M} + 1 \qquad \text{(II-36)}$$

According to Equation (II-34) the index of refraction for the combination of gases A and B now becomes

$$n = \frac{3}{2} \frac{\rho_A N_A}{M_A} + \frac{3}{2} \frac{\rho_B N_B}{M_B} + 1 \qquad \text{(II-37)}$$

Since

$$\rho_A = M_A c_A \tag{II-38A}$$

$$\rho_B = M_B c_B \tag{II-38B}$$

and

$$c = c_A + c_B \tag{II-39}$$

Equation (II-37) can be rewritten as

$$n = \left(\frac{3}{2} N_A - \frac{3}{2} N_B \right) c_A + \frac{3}{2} N_B c + 1 \tag{II-40}$$

Differentiating with respect to z and dropping the deviative of the constant molar density, c, gives

$$\frac{\partial n}{\partial z} = \frac{3}{2} (N_A - N_B) \frac{\partial c_A}{\partial z} \tag{II-41}$$

Discussion in Chapter IV will show that for the differential interferometer, the gradient of the index of refraction is proportional to the shift in the parallel fringe pattern. From Equation (IV-4)

$$\frac{\partial n}{\partial z} = \left[\frac{\lambda}{2Lg(n_e - n_o)\theta} \right] m \tag{II-42}$$

The quantity within the brackets consists of optical parameters and m is the fringe deflection. Substituting this result into Equation (II-41)

yields

$$\frac{3}{2}(N_A - N_B)\frac{\delta c_A}{\delta z} = \left[\frac{\lambda}{2Lg(n_e - n_o)\theta}\right] m \qquad \text{(II-43)}$$

Utilizing the equation of state for an ideal gas and rearranging Equation (II-43) gives

$$\frac{\delta x_A}{\delta z} = \left[\frac{\lambda}{Lg(n_e - n_o)\theta}\right]\left[\frac{\bar{R}T}{3P(N_A - N_B)}\right] m \qquad \text{(II-44)}$$

Equation (II-33) combined with Equation (II-44) now may be expressed as

$$D_{AB} = \frac{(1-x_{AO})^2 Q^2 \exp(Q^2)}{(t_b - t_a)}\left[\frac{3Lg(n_e - n_o)\theta P(N_A - N_B)}{\lambda \bar{R}T}\right]^2$$

$$\left[\left(\frac{1}{\exp[(E-Q)^2]m}\right)_b^2 - \left(\frac{1}{\exp[(E-Q)^2]m}\right)_a^2\right] \qquad \text{(II-45)}$$

Equation (II-45) is not readily solved for D_{AB} since E is a function of not only D_{AB} but also absolute time. Theoretically, the diffusion process is started instantaneously giving a definite instant for which t = 0. However, the test procedure required a finite time to extract the cover plate and start the evaporation of the exposed liquid. This initiation time produces uncertainty in absolute time and a corresponding potential error in the measured value of D_{AB}.

The initial attempt to overcome this problem made the assumption that the fringe deflection measurements would be made at the liquid-gas interface. If z = 0 then E = 0 and Equation (II-45) may be simpli-

fied to

$$D_{AB} = \frac{(1 - x_{AO})^2 Q^2}{(t_b - t_a)} \left[\frac{3Lg(n_e - n_o)\theta P(N_A - N_B)}{\lambda \bar{R} T} \right] \left[\left(\frac{1}{m_{bO}} \right)^2 - \left(\frac{1}{m_{aO}} \right)^2 \right] \quad \text{(II-46)}$$

In this equation D_{AB} becomes a function of only relative time, two fringe shift measurements at the interface and the physical and optical values required for any solution. However, the duplication edge (see Chapter IV) makes observation of the evaporating interface impossible. This difficulty necessitated a solution using absolute time or observation of the fringes away from the interface.

An attempt to produce a solution by using absolute time produced diffusivity values which were unacceptably far from expected results. Zero time was arbitrarily selected to be the time at which the cover plate was one-half extracted. A set of correction curves was generated using the absolute time to enable iteration for D_{AB} in this attempted solution.

The possible solution of Equation (II-45) can be accomplished by determining a method for evaluating E without a knowledge of either D_{AB} or absolute time. The method uses fringe deflection measurements at two different distances from the surface, z_1 and z_2, at two different times, t_a and t_b. Recall Equation (II-30)

$$\left(1/\frac{\partial E}{\partial z} \right) = \frac{-2 \exp[-(E - Q)^2]}{\sqrt{\pi}\,(1 + \operatorname{erf} Q)(\partial X/\partial z)} \quad \text{(II-30)}$$

Combining Equations (II-32) and (II-44) gives

$$\frac{\delta X}{\delta z} = \frac{1}{x_{AO}} \left[\frac{\lambda}{2Lg(n_e - n_o)\theta} \right] \left[\frac{2\bar{R}T}{3P(N_A - N_B)} \right] m \qquad \text{(II-47)}$$

When the two equations above are combined and rearranged they yield

$$\frac{\delta E}{\delta z} = \frac{-\sqrt{\pi}}{2} (1 + \text{erf } Q) \frac{1}{x_{AO}} \left[\frac{\lambda \bar{R}T}{3Lg(n_e - n_o)\theta P(N_A - N_B)} \right] \exp[(E-Q)^2] m \qquad \text{(II-48)}$$

where

$$\frac{-\sqrt{\pi}}{2} (1 + \text{erf } Q) \frac{1}{x_{AO}} \left[\frac{\lambda \bar{R}T}{3Lg(n_e - n_o)\theta P(N_A - N_B)} \right] = \text{constant} = K_3 \qquad \text{(II-49)}$$

for a given test. Thus, at a given time t

$$\frac{\delta E}{\delta z}\Big|_t = K_3 \exp[(E - Q)^2] m \qquad \text{(II-50)}$$

Then for the two distances above the interface z_1 and z_2 at given time t

$$\frac{\delta E}{\delta z}\Big|_{t,z_1} = K_3 \exp[(E(z_1) - Q)^2] m_{z_1} \qquad \text{(II-51A)}$$

$$\frac{\delta E}{\delta z}\Big|_{t,z_2} = K_3 \exp[(E(z_2) - Q)^2] m_{z_2} \qquad \text{(II-51B)}$$

These two expressions must be equivalent since for the given time t from definition

$$E = \frac{z}{\sqrt{4D_{AB}t}} \qquad \text{(II-52)}$$

Taking the derivative with respect to z yields

$$\left.\frac{\partial E}{\partial z}\right|_t = \frac{1}{\sqrt{4D_{AB}t}} \neq \text{function}(z) \qquad \text{(II-53)}$$

which is constant for invariant D_{AB} at a given time. Thus expressions (II-51A) and (II-51B) are equal and

$$\exp[(E(z_1)-Q)^2]m_{z_1} = \exp[(E(z_2)-Q)^2]m_{z_2} \qquad \text{(II-54)}$$

Also at the given time t for z_1 and z_2 from the definition of E

$$E(z_1) = \frac{z_1}{\sqrt{4D_{AB}t}} \qquad \text{(II-55A)}$$

$$E(z_2) = \frac{z_2}{\sqrt{4D_{AB}t}} \qquad \text{(II-55B)}$$

Thus by combining

$$E(z_1) = E(z_2)\left(\frac{z_2}{z_1}\right) \qquad \text{(II-56)}$$

Substituting this expression into Equation (II-54), taking the logarithm of both sides, and rearranging yields for time t

$$E^2(z_1)\left[1 - \left(\frac{z_2}{z_1}\right)^2\right] - E(z_1)\left[2Q - 2\left(\frac{z_2}{z_1}\right)Q\right]$$

$$- \ln\left(\frac{z_2}{z_1}\right) = 0 \qquad \text{(II-57)}$$

which is a quadratic equation in $E(z_1)$. This equation may be solved for $E(z_1)$ if the two vertical distances, z_1 and z_2 and the corresponding fringe shifts at those levels, m_{z_1} and m_{z_2}, are known. The solution results in a correction factor, r, that is applied to the fringe deflection measured at the top of the duplication edge where $z = z_1$. The factor is of the form

$$r_{z_1} = \frac{\exp[(E(z_1) - Q)^2]}{\exp[Q^2]} \qquad \text{(II-58)}$$

The corrected fringe deflection becomes

$$m_{cr} = m\, r_{z_1} \qquad \text{(II-59)}$$

Equation (II-45) for diffusivity now is

$$D_{AB} = \frac{(1-x_{AO})^2 Q^2}{t_b - t_a}\left[\frac{3L g(n_e - n_o)\theta P(N_A - N_B)}{\lambda \bar{R} T}\right]^2\left[\left(\frac{1}{m_{cr}}\right)_b^2 - \left(\frac{1}{m_{cr}}\right)_a^2\right] \qquad \text{(II-60)}$$

The working form of this equation that was used in the data reduction is

$$D_{AB} = (1 - x_{AO})^2\, Q^2\, K^2\, P_{tr} \qquad \text{(II-61)}$$

where

$$K = \frac{3Lg(n_e - n_o)\theta P(N_A - N_B)}{\lambda \bar{R} T} \qquad \text{(II-62)}$$

and P_{tr} is the test result parameter

$$P_{tr} = \frac{1}{t_b - t_a} \left[\left(\frac{1}{m_{cr}} \right)_b^2 - \left(\frac{1}{m_{cr}} \right)_a^2 \right] \qquad \text{(II-63)}$$

CHAPTER III

EVALUATION OF PHYSICAL AND OPTICAL PARAMETERS

Several of the parameters in Equation (II-60) are constant for all the test runs. They are:

$L = 35.66$ cm = test cell length

$g = 100.0$ cm = focal length of the spherical mirrors in the differential interferometer

$n_e - n_o = 0.00911$ = difference in index of refraction of the extraordinary and ordinary rays in the Wollaston Prism material.

$\lambda = 5820\ \mathring{A}$ = test wavelength

$\bar{R} = 82.054\ \frac{\text{atm - ml}}{\text{g-mole }^{\circ}\text{K}}$ = universal gas constant

The test cell length was determined by fully assembling the cell and measuring the glass to glass distance with a large vernier caliper. The test wavelength and the mirror focal length were obtained from technical information about the interferometer supplied by the manufacturer [57]. The index of refraction increment, $n_e - n_o$, was determined by plotting the value of this parameter as a function of the wavelength and interpolating for the value at the test wavelength. All of the remaining terms in Equation (II-60) vary from test to test.

The determination of the values of the atmospheric pressure, P, atmospheric temperature, T, Wollaston Prism angle, θ, equilibrium mole fraction, x_{AO}, dimensionless molar average velocity, Q, and the molar refractivities, N_A and N_B will be discussed in the remainder of this

chapter. The determination of $(t_a - t_b)$ and the fringe deflections, m_a and m_b, will be discussed in the data reduction section.

Equilibrium Mole Fraction

The assumption that the mole fraction at the interface was equal to the equilibrium mole fraction was used in Chapter II. Although the system is not at equilibrium during the tests, deviations from equilibrium in the vicinity of the interface are small except in the case of extremely high evaporation rates [24, 70]. Profcceding on this result, for ideal gases

$$x_{AO} = \frac{Pv}{P} \qquad \text{(III-1)}$$

Thus the determination of the mole fraction at the interface requires a knowledge of the vapor pressure of the evaporating component at its surface.

A great quantity of vapor pressure data are available from a number of references [19, 20, 34, 41, 42, 72, 74]. Stoll [59] presents an extensive listing of vapor pressures as functions of temperature that have been obtained experimentally. All substances selected for diffusivity measurements were chosen from those which had vapor pressure data appearing in Reference [59]. The temperature of the liquid-gas interface was recorded during all tests by a thermocouple approximately .1mm from the liquid's surface. The mean interface temperature during the test was used to determine the vapor pressure from plots of the data previously discussed. The ambient pressure was measured by a barometer and corrected for temperature. The ratio of the equilibrium

surface vapor pressure to the atmospheric pressure was then equated to the interface equilibrium mole fraction.

The dimensionless molar average velocity, Q, arises in the transformation of Equation (II-10) and is defined to be

$$Q = \frac{x_{AO} \exp[-Q^2]}{(1 - x_{AO})\sqrt{\pi}\,(1 + \text{erf } Q)} \qquad \text{(III-2)}$$

which may be rearranged to

$$x_{AO} = \frac{1}{1 + \dfrac{1}{\exp[Q^2]\, Q\, \sqrt{\pi}\,(1 + \text{erf } Q)}} \qquad \text{(III-3)}$$

Thus, once the equilibrium interface mole fraction has been evaluated, a value of Q may be determined. Since Equation (III-3) is implicit in Q and quite awkward, a plot was made of the values of Q as a function of x_{AO} from Reference [3] plus additional values of the parameters generated using Equation (III-3) to insure the curve was faired correctly. The scales on the plot were chosen to make the determination of Q as a function of x_{AO} very accurate when the graph was read. This method was found to be sufficiently accurate and much less time consuming that iterating Equation (III-3) for a value of Q. Care had to be taken in the evaluation of Q and x_{AO} since a small error in the determination of Q was found to cause appreciable change in the value of the diffusivity.

Molar Refractivities

The molar refractivity of air, N_B, was obtained as follows. The Lorenz-Lorentz equation for air is

$$N_B = \frac{n_B^2 - 1}{n_B^2 + 2} \frac{\bar{R}T_B}{P} \qquad \text{(III-4)}$$

where T_B are P are respectively the air temperature and pressure. The index of refraction of air, n_B, is dependent upon the air temperature, pressure, and relative humidity. The correction factor for relative humidity is given by Reference [74] to be,

$$(n_B - 1) = (n_{DB} - 1) - \frac{0.41\, x_{wv}}{10^4} \qquad \text{(III-5)}$$

where n_{DB} is the index of refraction of dry air and x_{wv} is the mole fraction of water vapor in the air. Since the air is assumed to be an ideal gas, the mole fraction is the ratio of the water vapor partial pressure to the total pressure

$$x_{wv} = \frac{P_{wv}}{P} \qquad \text{(III-6)}$$

The partial pressure of the water vapor was determined from a psychrometric chart using measured values of the wet and dry bulb temperatures.

The correction factor for temperature and pressure has the form

$$(n_{DB} - 1)_{T,P} = (n_{DB} - 1)_r \frac{P}{P_r} \frac{T_r}{T} \qquad \text{(III-7)}$$

Combining Equations (III-5), (III-6), and (III-7) yields

$$n_B = 1 + (n_{DB} - 1)_r \frac{P}{P_r} \frac{T_r}{T} - \frac{0.41\ P_{wv}}{10^4\ P} \qquad \text{(III-8)}$$

which contains the corrections for pressure, temperature, and the presence of water vapor in the air.

Reference [74] contains dry air index of refraction data for a reference temperature of 288°K and a reference pressure of 1.0 atmosphere (760 mm). A straight line interpolation was used to determine $(n_{DB} - 1)$ at the interferometer wavelength to be 0.00027658. The equation used to determine now becomes

$$n_B = 1 + 0.00027658 \frac{P}{(760)} \frac{(288)}{T_B} - \frac{0.41\ P_{wv}}{10^4\ P} \qquad \text{(III-9)}$$

where P is in mm of Mercury and T is in °K. Using the assumption that

$$\frac{n^2 - 1}{n^2 + 2} \simeq \frac{2}{3} (n - 1) \qquad \text{(III-10)}$$

The Lorenz-Lorentz Equation, (III-4) becomes

$$N_B = \frac{2\ \overline{R}T_B}{3P} \left[0.00027658 \frac{P}{(760)} \frac{(288)}{T_B} - \frac{0.41\ P_{wv}}{10^4\ P} \right] \qquad \text{(III-11)}$$

which was the form used in computing the molar refractivity of air. The humidity correction was found to be on the order of only 0.3 percent and could be omitted if desired with little loss in accuracy.

The molar refractivity of the evaporating substance, N_A, was

also calculated using the Lorenz-Lorentz Equation in the form

$$N_A = \frac{n_A^2 - 1}{n_A^2 + 2} \frac{M_A}{\rho_A} \qquad \text{(III-12)}$$

For all the reference substances, data for the index of refraction and density are available from Reference [72] in which optical data are presented at four different wavelengths, 4340.6 Å, 4861.5 Å, 5893.0 Å, and 6563.0 Å for the substances in the liquid state. However, the molar refractivity is very nearly independent of phase, temperature, and pressure. This enables the use of the liquid phase data for values in the vapor phase. In order to obtain the molar refractivity at the test wavelength, the values at the four available wavelengths were computed using Equation (III-12) and plotted. The molar refractivity at λ = 5820.0 Å was then interpolated from graphs similar to that shown in Figure 2.

For most of the substances of unknown diffusivity, the index of refraction was available at only λ = 5893.0 Å from Reference [74]. A method of correcting N_A to the test wavelength of 5820.0 Å was necessary. Figure 2 shows that the variation in molar refractivity decreases with increasing wavelength. The average difference in the molar refractivities for the two wavelengths (5893 Å and 5820 Å) for the reference substance was less than 0.08 percent. The greatest difference was 0.1 percent and the smallest difference was 0.06 percent. Thus, the value of molar refractivity at 5893.0 Å of an unknown substance could be corrected using the average difference with reasonable assurance that the error would be insignificant.

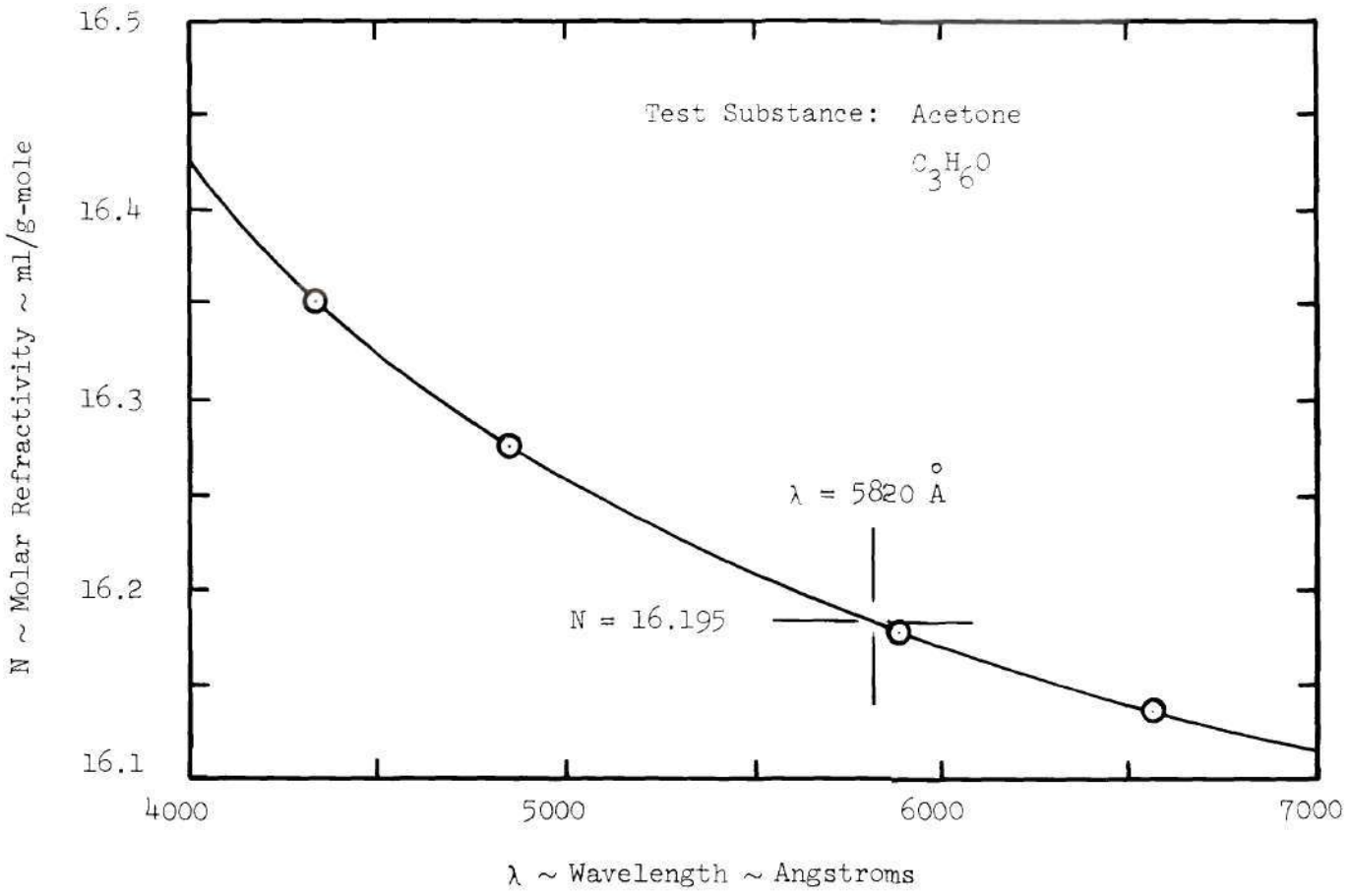

Figure 2. Variation of Molar Refractivity with Test Wavelength

Selection of Test Substances

Since not all volatile fluids are suitable for interferometric study, certain conditions had to be satisfied before potential test materials were considered acceptable. Two groups of test materials were selected. Materials referred to as reference substances were those with well established diffusivities and complete optical data available from the literature. Materials referred to as unknown substances were those with diffusivities previously undetermined experimentally. The conditions for selection of both reference and unknown test substances were:

1. Vapor pressure data as a function of temperature had to be available.

2. Sufficient optical data were necessary. All reference substances had index of refraction given at the four wavelengths listed previously. This enabled accurate computation of the molar refractivity. The reference substances were to be used to determine the accuracy of the interferometric method under consideration and were selected, in part, because of the completeness of existing information. Considerably less data were available for the substances of unknown diffusivity making necessary the application of the correction procedure previously discussed.

3. Since there is more experimental diffusivity data available for non-polar substances, only polar materials were selected as unknowns. The reference substances with two exceptions were also polar.

4. Substances of only moderate toxicity could be investigated in this study due to lack of ventilation in the laboratory. No venting was possible in the interferometer area since the air in the laboratory

had to be still during the tests to avoid possible disruption of the fringe patterns. Toxicity data were found in References [25] and [30].

5. Reference substances needed well documented diffusivities so that comparison with experimental results would be meaningful. Unknown substances should have undetermined diffusivities. It is, of course, impossible to state categorically that the diffusivities of the substances selected as unknowns have not been experimentally determined. Values for their diffusivities have not been published in any of the major sources of diffusivity data [39, 40, 47, 51, 68, 72] and to the best of the author's knowledge have not been previously determined experimentally.

The materials selected for potential investigation were:

Name	Chemical Formula	Type of Substance	Polarity
1. Toluene	C_7H_8	Reference	Non-polar
2. n-Hexane	C_6H_{14}	Reference	Non-polar
3. Methanol	CH_4O	Reference	Polar
4. Acetone	C_3H_6O	Reference	Polar
5. Methyl Acetate	C_3H_6O	Reference	Polar
6. Methyl Propionate	$C_4H_8O_2$	Reference	Polar
7. Ethyl Formate	$C_3H_6O_2$	Reference	Polar
8. Dibromomethane	CH_2Br_2	Unknown	Polar
9. 1-Chloropropane	C_3H_7Cl	Unknown	Polar
10. 2-Chloropropane	C_3H_7Cl	Unknown	Polar
11. Vinyl Acetate	$C_4H_6O_2$	Unknown	Polar
12. 2-Chlorobutane	C_4H_9Cl	Unknown	Polar

Name	Chemical Formula	Type of Substance	Polarity
13. 1-Chloro-2-methyl-propane	C_4H_9Cl	Unknown	Polar
14. 2-Chloro-2-methyl-propane	C_4H_9Cl	Unknown	Polar
15. Butyl Formate	$C_5H_{10}O_2$	Unknown	Polar
16. Propylene Oxide	C_3H_6O	Unknown	Polar
17. Butyl Bromide	C_4H_9Br	Unknown	Polar

All of the above substances are clear or slightly yellow, highly inflammable liquids at room temperature. Toxicity of those fluids for which data were available is low to moderate. Several of the substances were of unknown toxicity.

Before making the final selection of the test substances, each candidate was evaluated to see if its combination of volatility and molar refractivity would produce sufficient fringe deflection for accurate diffusivity measurement. Recall Equations (II-30), (II-32), and (II-44)

$$\left(1/\frac{\delta E}{\delta z}\right) = \frac{-2\ \exp[-(E-Q)^2]}{\sqrt{\pi}\ (1 + \text{erf}\ Q)(\delta X/\delta z)} \qquad \text{(II-30)}$$

$$\frac{\delta X}{\delta z} = \frac{1}{x_{AO}} \frac{\delta x_A}{\delta z} \qquad \text{(II-32)}$$

$$\frac{\delta x_A}{\delta z} = \frac{\lambda}{Lg(n_e - n_o)\ \theta} \frac{\bar{R}T}{3P(N_A - N_B)}\ m \qquad \text{(II-44)}$$

Combining the above three equations and the derivative of E with respect to z from the definition

$$\frac{\partial E}{\partial z} = \frac{1}{\sqrt{4 D_{AB} t}} \qquad \text{(III-13)}$$

yields, when solved for fringe shift

$$m = \frac{3\ Lg(n_e - n_o)P}{2\ \bar{R}T\ \sqrt{\pi}} \left[\frac{(N_A - N_B)\ x_{AO}}{(1 + \text{erf}\ Q)\ \exp[E-Q)^2]\ \sqrt{D_{AB} t}} \right] \theta \qquad \text{(III-14)}$$

A set of conditions that might occur during a test was then assumed. Further, for ease of calculation, E was assumed equal to zero (corresponding to a condition of z = 0) and $D_{AB} = 0.09\ cm^2/sec$ which is a nominal value for the type of substances under consideration. The assumption that E = 0 can change the estimated fringe shift by up to $\Delta m = 2$. Since the estimation was qualitative, an error of this magnitude was of little consequence. With these assumptions made, and with the use of the nominal test condition data, the expression for fringe shift became

$$m \tilde{=} \text{constant} \left[\frac{(N_A - 4.37)\ x_{AO}}{(1 + \text{erf}\ Q)\ \exp[Q^2]\ \sqrt{t}} \right] \theta \qquad \text{(III-15)}$$

Equation (III-15) was used initially to determine which of the three interferometric sensitivity settings was to be used for each substance. An arbitrary time of one second was used in conjunction with the assumed test conditions to produce an estimated fringe shift for

each substance for each of the three Wollaston Prism settings. The prism that produced at least ten and preferably less than twenty fringe shifts at one second into the test was selected for use in the test runs.

The equation was also used to check the selected camera speed setting. If the number of fringe shifts changed very rapidly with time, a higher camera speed was necessary to prevent blurring of the fringes. The estimated times for the appearance of thirty, twenty, and ten fringe shifts were calculated for each substance. These data were then used to determine the appropriate camera speed. If the fringes were changing at a rate greater than one fringe shift per twenty frames exposed, the camera speed was increased.

CHAPTER IV

TEST EQUIPMENT

The data acquisition system consisted of a differential interferometer, high speed camera with timing devices, diffusion cell, and temperature measurement and recording equipment. The remainder of this chapter presents details of the various components of the test equipment used.

Differential Interferometer

A schematic diagram of the differential interferometer is shown in Figure 3. Brief descriptions of the operation of the differential interferometer may be found in References [6] and [7] and a more extensive description in Reference [15].

Light leaving the light source (LS) first passes through a filter (5820 $\mathring{A}$ used in this work). The light travels through a collecting lens (L1) followed by a polarizer (P) which produces equal magnitude electric vectors. These components are focused on the first of three Wollaston Prisms (WP1) which causes the two components to diverge slightly as they leave the prism forming two separate rays. The Wollaston Prism is located at the focal point of the first spherical mirror (SM1). Thus, when the two rays reach the test section they follow parallel paths separated by a small lateral displacement referred to as the separation distance, Δz, where

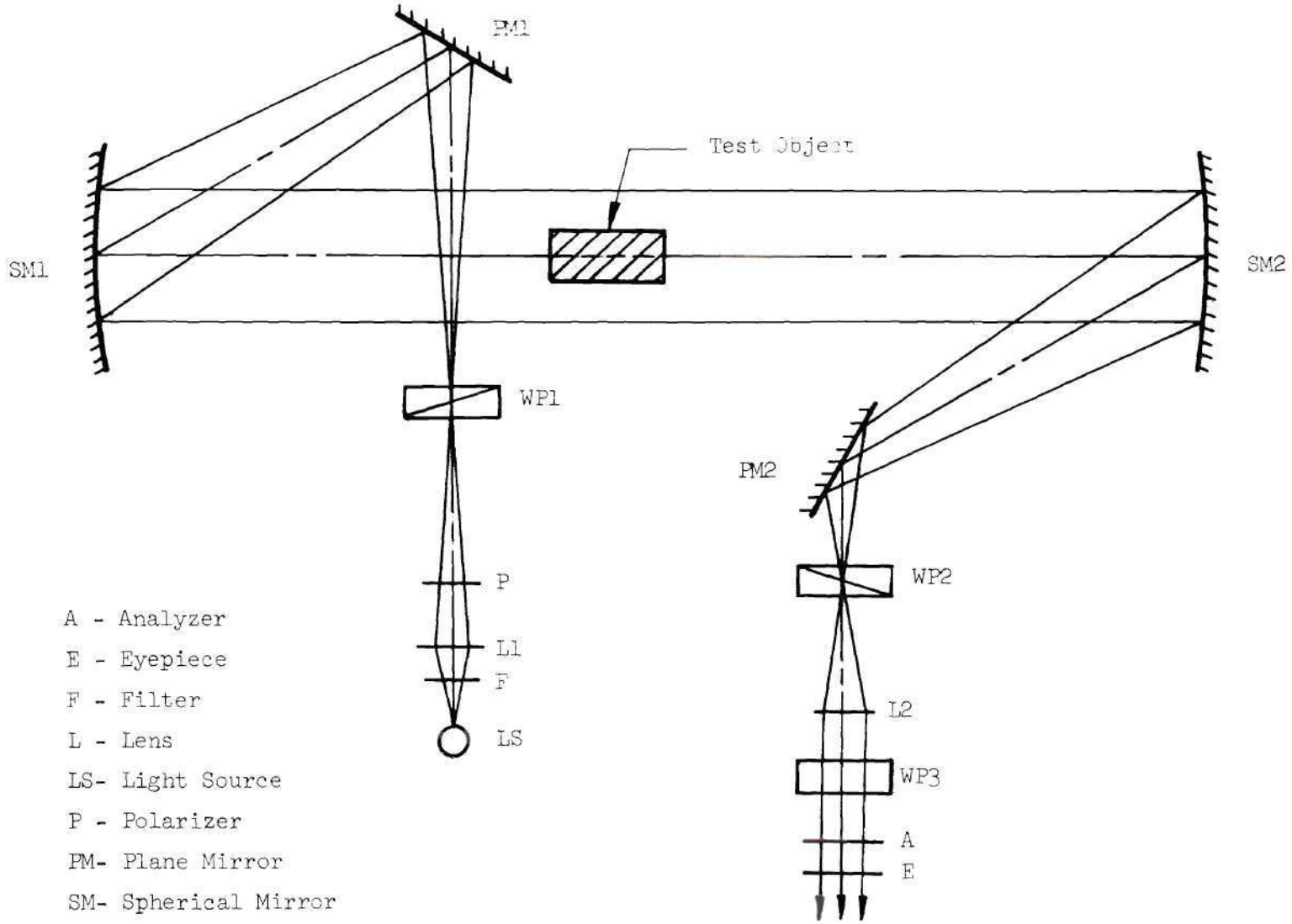

Figure 3. Schematic Diagram of a Differential Interferometer

$$\Delta z = 2g(n_e - n_o)\ \theta \qquad \text{(IV-1)}$$

and

g = focal length of the spherical mirror

$(n_e - n_o)$ = difference in index of refraction between extra-ordinary and ordinary rays in the Wollaston Prism material.

$\theta \cong \tan\theta$ = tangent of Wollaston Prism angle.

Since the two separated rays pass through different regions in the test section, they experience different optical paths, ϕ, due to the variation in concentration of the diffusing vapor within the test cell. The difference in optical paths experienced by the two electric vector components can be expressed as

$$\Delta\phi = \Delta(nL) = L\Delta n = m\lambda \qquad \text{(IV-2)}$$

where

L = length of diffusion channel in the direction of light propagation

n = index of refraction of air at wavelength λ

m = number of fringe shifts

After passing through the test section, the rays are focused by the second spherical mirror (SM2) on the second Wollaston Prism (WP2). The second prism has been rotated 180° with respect to the first Wollaston prism so that its effect on the rays is to reverse the action

of the first prism and to recombine the two rays into a single ray. The light then passes through a third Wollaston prism (WP3) which produces a phase shift between the two electric vector components. As the combined rays pass through the analyzer (A), interference is produced. The interference pattern appears as alternate light and dark bands which are deflected in the regions where there is a difference in optical path encountered in the test section.

Since the separation distance, Δz, is very small, the ratio of the change in index of refraction to the separation distance closely approximates the gradient in index of refraction.

$$\frac{\Delta n}{\Delta z} \simeq \frac{\partial n}{\partial z} \qquad \text{(IV-3)}$$

When Equations (IV-1), (IV-2) and (IV-3) are combined an expression for gradient in index of refraction as a function of optical parameters and fringe shift may be obtained.

$$\frac{\partial n}{\partial z} = \left[\frac{\lambda}{2\ Lg(n_e - n_o)\ \theta} \right] m \qquad \text{(IV-4)}$$

Equation (IV-4) is used in Chapter II to convert the theoretical expression for diffusivity to one in terms of measurable test parameters.

The differential interferometer used in this study was constructed in a manner that allows the rotation of the polarizer, Wollaston prisms and analyzer. Rotation of the interferometer arm containing the polarizer and first Wollaston prism allows the plane containing the two

parallel rays to intersect the test section at any angle. When the other arm containing the second and thrid prisms and the analyzer is rotated to the recombining position, the gradient in index of refraction may be measured in any arbitrary direction. The positions of the arms are coupled in that the second arm must be positioned to exactly reverse the ray splitting action of the first arm.

The interferometer is equipped with three sets of Wollaston prisms attached to selector mechanisms. The prisms have angles of one, three, and eight degrees. Equation (IV-4) shows that the number of fringe shifts produced by a given concentration gradient is directly proportional to the Wollaston prism angle, θ. Thus, selecting different prisms allows for a variation in sensitivity to fit individual test conditions.

Inherent in the optics of the differential interferometer is the formation of a double image which is referred to as a duplication edge. The duplication edge is the result of the blocking by the test object of one of the paired rays passing through the test section. Figure 4 schematically illustrates this phenomenon. It may be seen from the figure that one component of rays 2 and 3 has been blocked by the test object. When the rays are recombined after exiting the test section, a region of reduced illumination will appear where only one component has passed through. A gray area is thus produced which is of a thickness equal to the separation distance, Δz, given by Equation (IV-1). It appears on all surfaces of the test object which have components normal to the plane containing the two separated rays. Since ray 1 in Figure 4 passes closest to the test object without having one

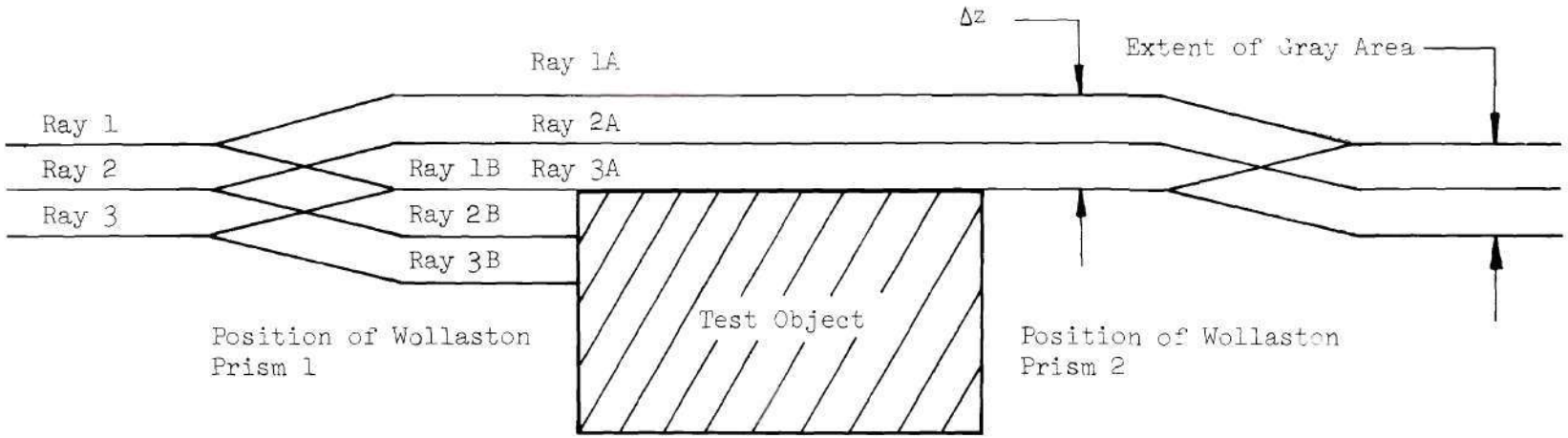

Figure 4. Blockage of Separated Rays by Test Object Producing Duplication Edge

component blocked, it is the first ray capable of detecting a gradient near the test surface. Thus, the gradient indicated by the number of fringe shifts at the top of the duplication edge is actually the gradient at a point $\Delta z/2$ away from the surface of the test object.

The interferometer was enclosed by a shield constructed for a free convection project. The back of the shield was removed to allow easier entry and exit of the test cell to the interferometer test section.

Camera and Timing Devices

The interferogram recording camera, mount, and timing equipment are shown in Figure 5. The camera was a Red Lake Laboratories Hy-Cam 16 mm High Speed model equipped with a 16 mm focal length lens. The film used was Kodak Reversal 7277, 16 mm high speed motion picture film. Camera frame speeds ranged between 100 and 160 frames per second. The camera was bolted to a mount which allowed sufficient freedom of movement to product a properly aligned and sized image on the film.

The camera was equipped with a neon flash tube for use with a timing system. This system consisted of a Red Lake Laboratories Milli-Mite Timing Light Generator Model TLG-3 and a Kepco Laboratories Regulated Power Supply. The Milli-Mite was calibrated using a Hewlett Packard digital counter and found (after an extended warm-up period) to produce a constant 100.4 pulses per second. Each pulse caused the neon flash tube to expose a small square on the edge of the film as it moved past the light. The indicator square did not interfere with the image on the film. Since camera fram speed was not constant during the acceleration and deceleration phases of operation, the indicators were used to determine the time between the interferograms selected for data reduction.

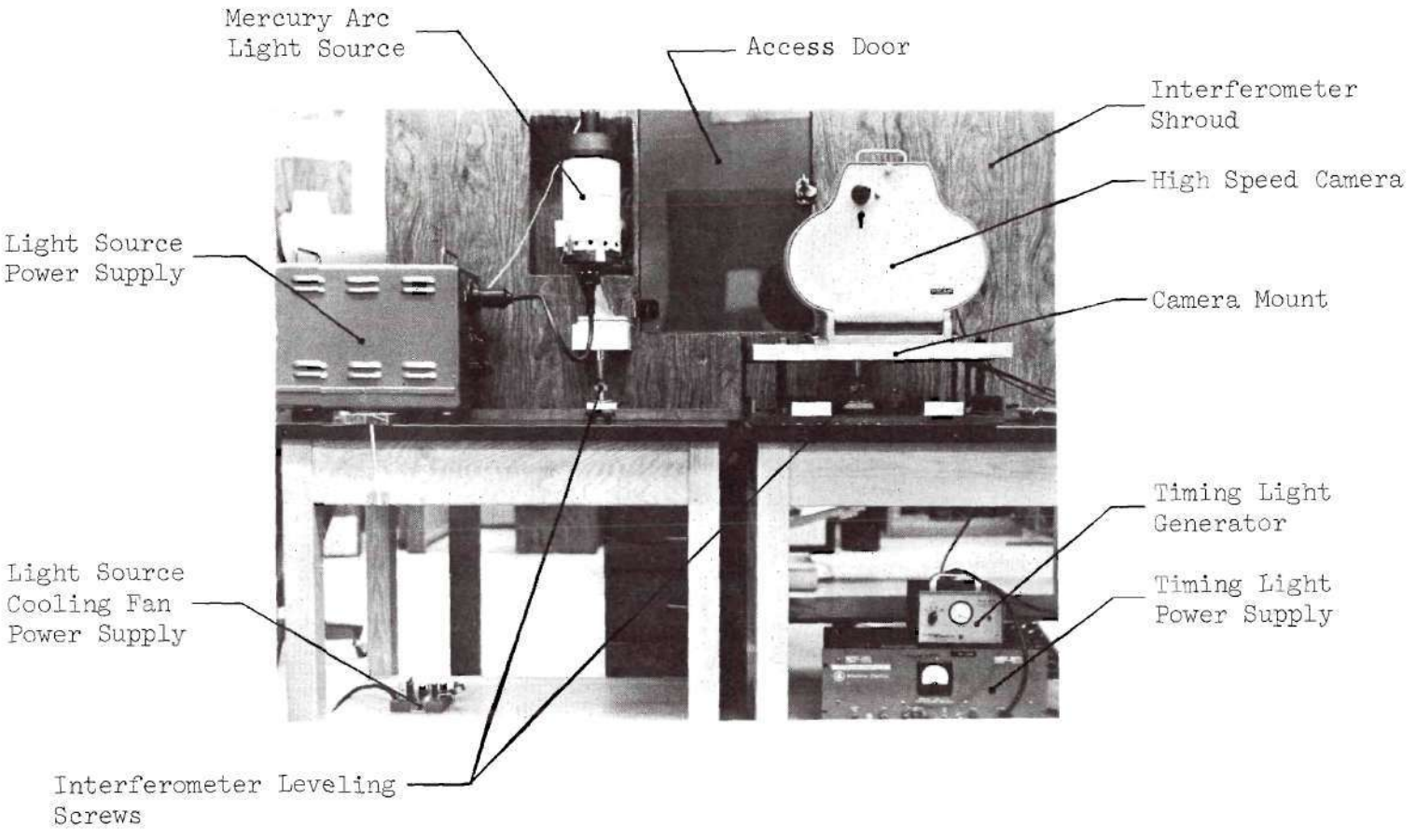

Figure 5. Interferometer, Camera, and Timing Equipment

Test Cell and Support Stand

The cell used in this study is schematically shown in a cross-sectional view in Figure 6. The cell body consisted of three main sections, a base plate and two 25.4 mm thick aluminum vertical walls that bolt to the base plate. The vertical walls each had two bolt-on flanges which were adjusted with shims to insure that the walls were parallel and 25.4 mm apart. The base plate was machined from a single piece of 25.4 mm thick aluminum stock. It contained a channel 25.4 mm wide and 3.18 mm deep for the test fluid.

A shim made of 0.51 mm thick stainless steel was used to cover the fluid in the channel before the evaporation process was initiated. The shim material was thick enough for sufficient rigidity but thin enough to avoid disruption of the air at the interface as it was extracted. The shim was clamped so that it rode in a trough in the base plate. This guide made it possible to withdraw the shim assembly from the cell without the shim jamming against the glass end plates. The shim was extracted by hand since Grob [26] in similar circumstances found that mechanical and electrical shim removal systems proved unsatisfactory.

Both vertical walls and the base plate contained seals to prevent premature leakage of the vapor into the test cell. The rear butt seal was made of 3.18 mm thick closed cell neoprene foam. The front wiper seals were made of 6.35 mm thick stock of the same type material. The lower front seal was cut in a trapezoidal shape and glued to a wooden support to help it maintain its shape as the shim was extracted. The upper, front seal was rounded to insure minimal air or vapor leakage

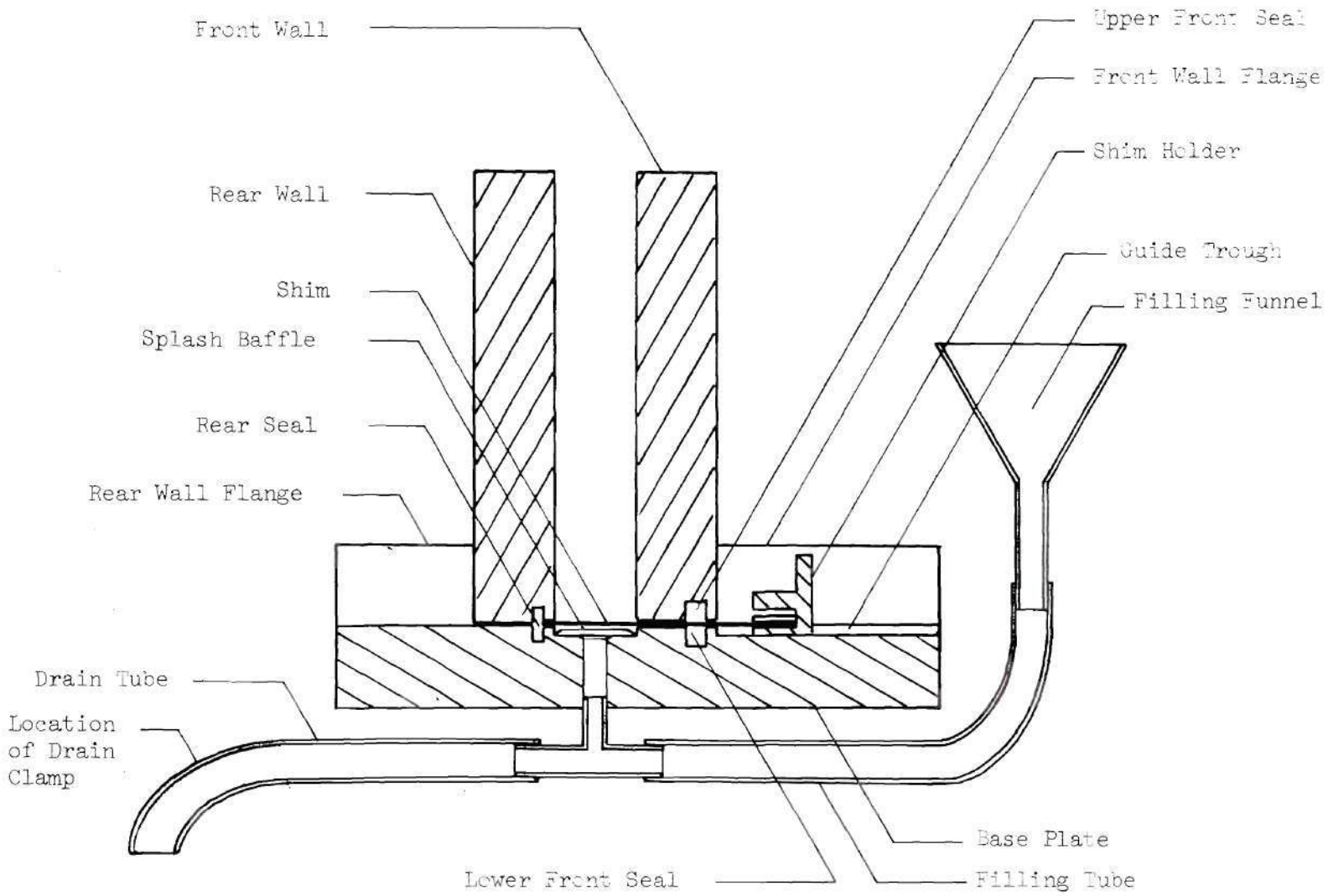

Figure 6. Schematic Cross Sectional Diagram of Test Cell

through the shim slot. Both front seals were always in contact with the shim. The end seals were cut from 0.4 mm thick neoprene sheet.

The ends of the cell were machined flat so that they provided a smooth surface to which the glass end plates could be clamped. The end plates were 6.35 mm thick poured plate glass. The poured plate, while not optically flat, proved suitable for use with the one and three degree Wollaston prism sensitivity settings. When the eight degree prisms were used, more significant deflections appeared in the fringe pattern due to the slightly irregular thickness of the glass. The end plates were held in place by five clamps on each end of the cell.

The test cell was mounted on the main supporting frame of the interferometer by means of four threaded members and a clamp system. This allowed adjustment of the cell in the field of view of the interferometer. The assembled test cell is shown on its support stand in Figure 7.

The amount of test fluid to be placed in the cell for a test was determined by carefully measuring the volume of the channel. This value is important because it determines the location of the liquid-air interface. It was found that the amount of fluid necessary to fill the channel (liquid surface flush with the top of the channel sides) was 27 ml. This volume was measured with a graduated cylinder before each test.

Three different methods were used to charge the cell with the liquid. Each method was a modification of a previous method in an attempt to improve the earlier techniques. The first two methods involved filling the channel from the top of the cell. They were unsatisfactory

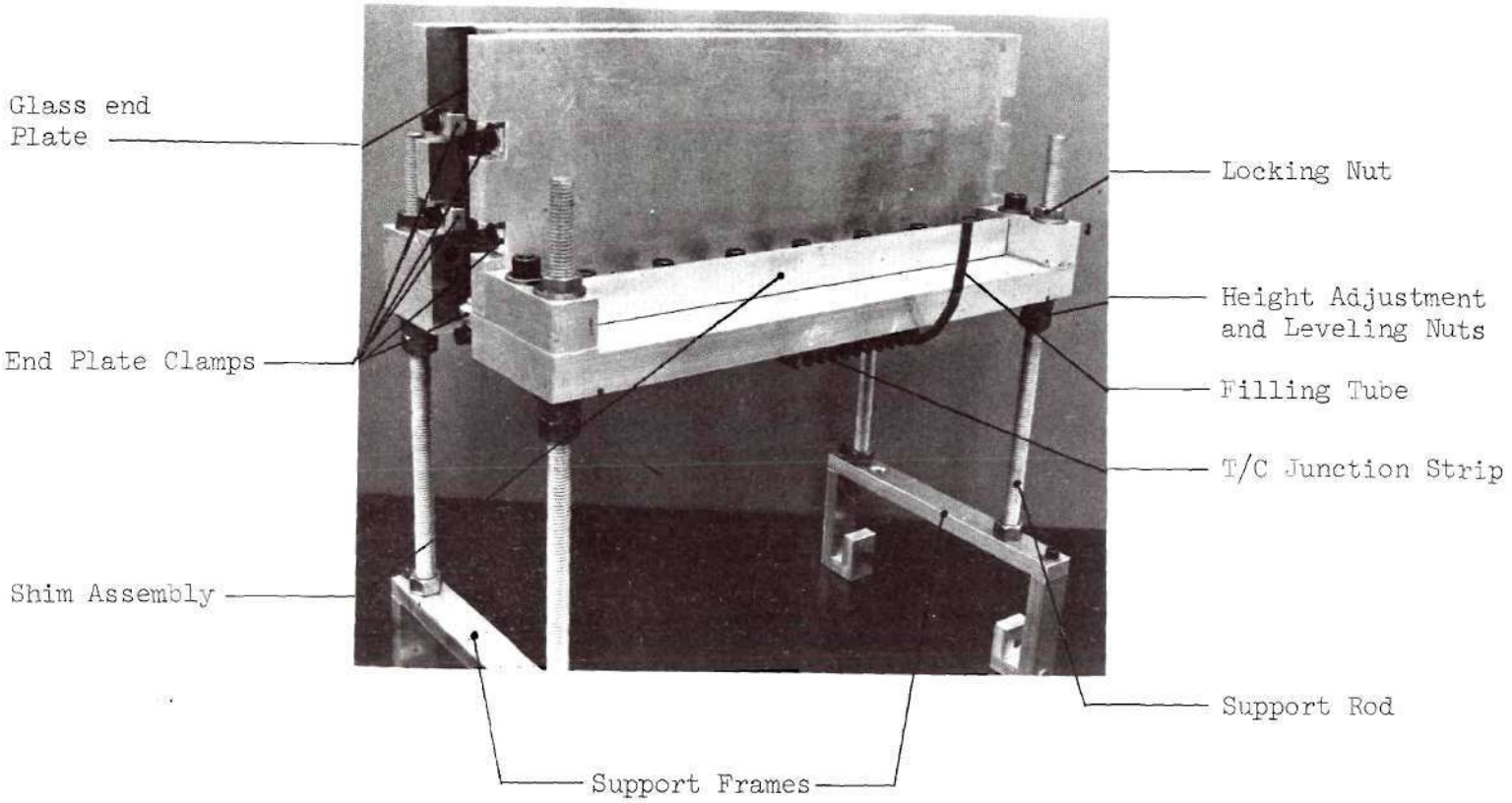

Figure 7. Test Cell on Support Stand

due to splashing of the test fluid and difficulty in clearing the cell of the vapor after inserting the shim. The third method, which gradually introduced the test liquid through a hole in the base plate, was found to minimize splashing, premature diffusion, and entrapment of air bubbles in the liquid. The filling system is shown in the schematic drawing of the cell in Figure 6.

The original design of the cell allowed the channel that was to hold the diffusing liquid to be machined the full length of the base plate. As a result, the liquid was able to come in contact with the glass end plates and by capillary action to wet the end plates, the rear seal, and eventually the shim. Therefore, the ends of the channel had to be sealed to avoid this problem. Several unsuccessful attempts were made before a solution was found which would avoid this problem. Additional material was milled away at the ends of the channel and 3.18 mm thick pieces of aluminum were simultaneously force fitted and glued in place with a silicone sealant. The tops of the end plates were then filed flush with the top of the base plate to allow viewing of the liquid-air interface. This modification proved satisfactory during preliminary testing, but gradual erosion of the original sealant by the test liquids eventually caused leakage problems. Also during preliminary tests, difficulties were encountered with the fluid coming in contact with the bottom of the shim. To correct this situation, additional spacers were placed under the flanges of the vertical walls. Another spacer was placed under the lower, front seal to force the shim to ride on the upper, front seal. The wetting problem was alleviated when the shim had been raised to a point 0.6 mm above the liquid surface.

Temperature Measurement and Recording

The need to measure test cell temperatures was twofold. First, the interface temperature and the air temperature immediately above the interface were parameters needed in the reduction of data. The interface temperature was used to determine the vapor pressure of the diffusing fluid, which, in turn, was used to evaluate the equilibrium mole fraction. The air temperature was used to determine the molar refractivity of the air in the cell. Second, the test cell temperatures were used to insure that the system had reached thermal equilibrium before initiating a test.

Five thermocouples (four in the cell and one external to the cell) were used in conjunction with a thermocouple selector switch, potentiometer and strip chart recorder to determine system temperatures. Thermocouple locations and nomenclature are shown schematically in Figure 8.

The liquid bulk and interface termocouples were made from 0.127 mm diameter, teflon coated, copper-constantan wire. They were inserted in a threaded plug and held in place by rubber-silicone sealant. The plug was removable for cleaning and replacement of the liquid thermocouples if necessary. The 0.3 mm bead of the interface thermocouple was located immediately below the surface of the liquid so that it would accurately determine the surface temperature. The liquid bulk thermocouple was located approximately 1.59 mm deep in the 3.18 mm deep channel. This thermocouple was used in the determination of equilibrium and was not required for data reduction. The liquid bulk thermocouple also served as a backup for the interface thermocouple as it could easily be relocated to a position near the surface.

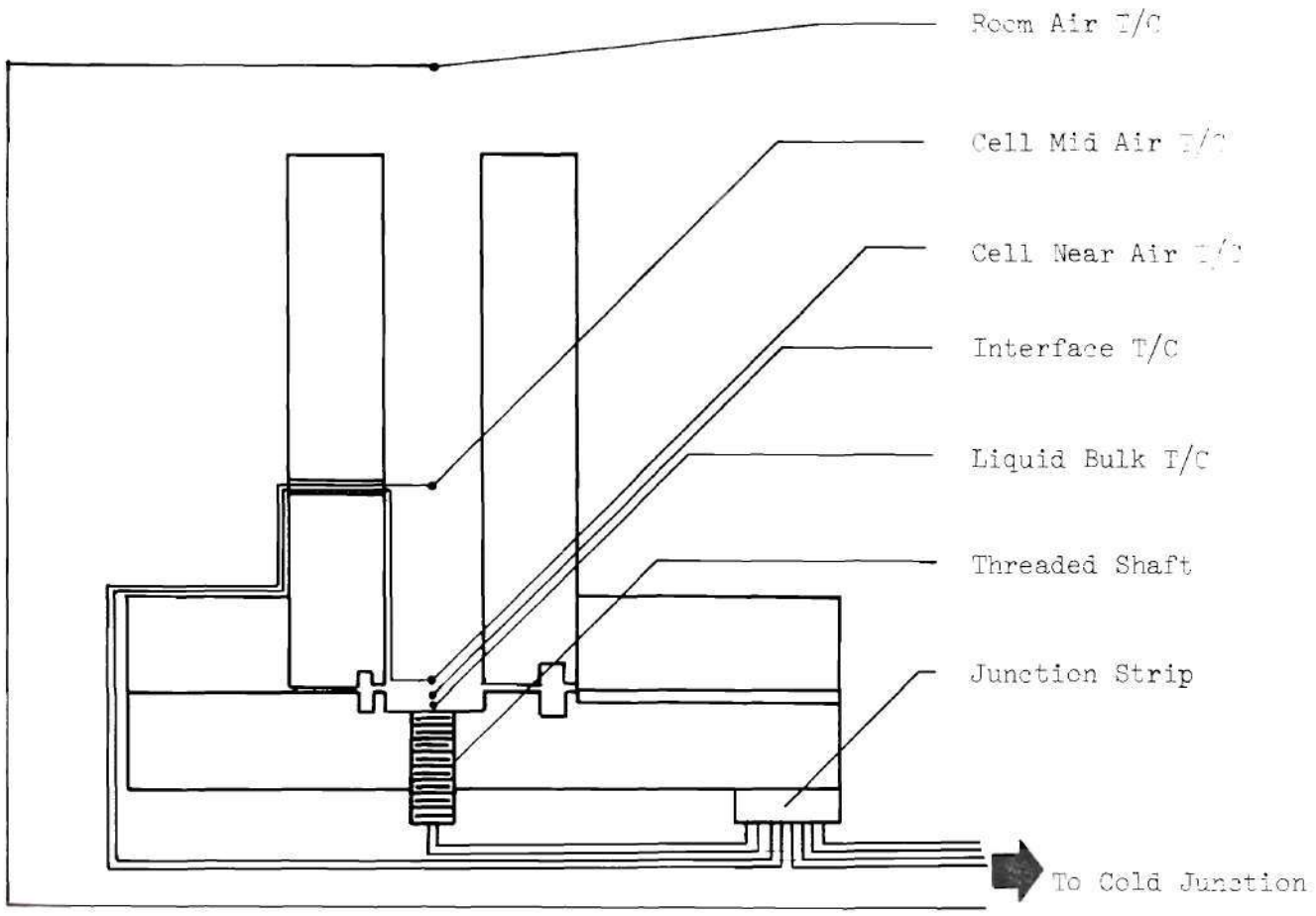

Figure 8. Test Cell Schematic Diagram Giving Thermocouple Locations and Nomenclature

Two air thermocouples were located in the cell as shown in Figure 8. The room air thermocouple was located outside of the cell. The near-air thermocouple was located immediately above the shim when the shim was in the closed position. The mid-air thermocouple was located approximately 50.00 mm above the interface. The leads for the two air thermocouples in the cell ran through a hole drilled in the rear vertical wall. All three air thermocouples were made from 0.254 mm diameter copper and constantan wire.

All the cell thermocouples were connected to a junction strip attached to the base plate. This allowed the thermocouple leads to be disconnected so that the cell could be removed from the interferometer for cleaning after each test. From the cold junctions the leads were connected to either a ten-way selector switch or to the strip chart recorder. The room-air thermocouple by-passed the junction strip and was routed directly to the ice-bath cold junction.

Two recorders were used during the tests. When available, a Moseley Autograph Model 7100BM dual pen strip chart recorder was used to monitor the interface and near-air temperatures continuously during the tests. The alternate recorder was a Leeds and Northrop ADJ AZAR single pen recorder. When only one recording channel was available, the interface temperature was recorded during the test since the vapor pressure is a stronger function of temperature than the molar refractivity.

The thermocouples that were not connected to the recorder were routed through the selector switch to a Leeds and Northrop Volt Potentiometer. The outputs of these thermocouples were manually measured and

recorded before and during each test. In addition to the above data, the wet and dry bulb temperatures in the laboratory were measured with a sling psychrometer after each test.

CHAPTER V

TEST PROCEDURE AND DATA REDUCTION

Test Procedure

Each new test series started with the cleaning of the test cell with distilled water to insure that no material from the previous test was present. After cleaning, the cell was completely dried before assembling. Next, the rear seal was inserted in its seat and the rear wall properly positioned. The rear wall was checked with a machinist's square to make certain it was perpendicular to the base plate. The locations of the liquid-bulk and interface thermocouples were then checked and adjusted if necessary.

Next, the lower front seal was positioned and lubricated with a small quantity of petroleum jelly. The shim assembly was then placed in the guide trough with the shim extending over the seal. The upper front seal was also lubricated and the front wall placed in position. Before the front wall was tightened, the separation of the walls was checked with a gauge block to insure the width of the diffusion path was 25.4 mm. The bolts holding the front wall in place were then secured and the shim pushed to the initial position in which it touched the rear seal. The clearance of the near-air thermocouple was checked to insure that it was as close as possible to the shim without touching.

The glass end plates were then cleaned with solvent. Next, the end seals were positioned, the glass placed over them, and clamped into

position with one end clamp. The position of each end seal was adjusted and the remaining end clamps tightened. The seals and clamps were then inspected again for possible interference with the passage of light through the cell. Tape was then placed over the gaps between the cell base plate and vertical walls and extended to the glass in an attempt to prevent leakage.

The high speed camera was loaded with film and the timing device checked for proper voltage input. The interferometer filter was removed allowing bright, full intensity, white light to pass from the light source into the test region of the interferometer.

The test cell was then placed on the support stand in the test section. The upper locking nuts were placed on the threaded shafts but not tightened. The leads to the four cell thermocouples were attached to the junction strip on the base of the cell and the cold junctions inserted in the ice bath. The cell was then pivoted on the support struts to align the vertical walls with the light passing through the test section. This was accomplished by observing the incidence of the light on the inner and outer surfaces of the front wall of the cell. Since the light-rays passing through the test region are theoretically parallel, the cell could be moved until only a small amount of scattered light was incident on either side of the front wall. The alignment was checked by observing the clarity of the inner edges of the cell walls, and by maximizing the observed distance between the cell walls as seen through the interferometer. The upper locking nuts were then tightened to fix the location of the cell and the test wavelength filter repositioned into the light path.

The cell was not aligned in the horizontal plane for each test. The support stand had two nuts under the cell on each of the four threaded shafts. Once the cell had been leveled the nuts were locked against each other to insure that they could not move. The leveling was therefore permanent.

The next step in the test procedure required the checking of the thermocouples to see if they were connected and working properly. Both the strip chart recorder and potentiometer were then calibrated and checked for proper operation.

The proper cell charge was then measured in a clean graduated cylinder and introduced into the cell. Concurrent visual observation and reading of the thermocouples were used to determine when equilibrium had been reached. The fringes were observed through the camera eyepiece to see if any deflection occurred near the surface. Any deflection of the parallel fringe pattern would indicate that the evaporating vapor was leaking around the covering shim or that vapor remained in the cell from the filling process. If the fringes were deflected, air was blown into the cell to remove any residual vapor. The temperatures were checked again since introducing compressed air into the cell upset the equilibrium.

A test would not be initiated until the potentiometer readings of the cell thermocouples were within the desired range of ± .001 mv from the mean. The temperatures of the interface and the air immediately above the shim were most critical since they were measured in the region where the data would be recorded. The initial (before pulling the shim) difference in these two temperatures never exceeded an indicated value of 0.05°K in the tests considered for data reduction.

When equilibrium was apparently reached within the cell, the camera was started and the shim withdrawn by hand to start the diffusion process. The camera was timed with a stop watch and allowed to run for a predetermined interval depending upon the volatility and molar refractivity of the test substance. The temperatures not being continuously recorded during the test were manually monitored and recorded during the test.

After the test was completed, the cell was drained of the remaining test liquid and removed to the cleaning and assembly area. The barometric pressure, the wet bulb, and the dry bulb temperatures required in the data reduction were then measured and recorded. This completed the procedure of each test series.

Data Reduction

The number of fringe shifts was determined by projecting the fringe pattern on a screen with an L/W Photo Optical Data Analyzer Model 224-A. The image on the screen was approximately ten times the size of the test cell.

Before any fringe measurements were made, the film of the entire test was viewed to determine if there was any sloshing of the fluid as the shim was removed or leakage of the vapor around the shim before its extraction. If neither of these malfunctions was observed and if the film displayed sufficient clarity, the test was evaluated to determine the fringe deflection as a function of time.

Usually from six to ten individual frames were selected for reduction. Whenever possible, the frame farthest from the beginning

of the test showed at least ten fringe shifts. This criterion for selection of the last (in time) interferogram to be analyzed resulted from a desire to minimize the error due to misreading of the fringe shift. This point will be discussed further in Chapter VI. The interferogram (selected for reduction) nearest the start of the test usually was the first frame of sufficient clarity for a reasonably accurate reading. Typically, for the more volatile test substances, the first frame reduced would have in excess of twenty fringe shifts. Between the end points, other frames were chosen at increments of approximately one fringe shift. The interferograms selected were marked and numbered for identification.

Two different procedures were used in the data reduction to determine the number of fringe shifts on a given interferogram. During the first few test series the cell was positioned lower in the interferometer's field of view than in subsequent tests. The view through the cell during the two groups of tests is shown in Figures 9 and 10.

When the shim was extracted, the fringes deflected sharply in the vicinity of the interface. It should be noted that theory (Equation III-15) predicts an infinite interface fringe shift at time t = 0. The deflection of the fringes then slowly proceeded up the cell while the large initial deflection near the surface of the liquid diminished. During reduction of the first group of tests, the longer length of the fringes allowed sighting along the undeflected portion of fringe with a large triangle. Figure 11 shows how the intersections of the undeflected fringes and the duplication edge were determined. Once the undeflected fringe positions were established, the total fringe shift

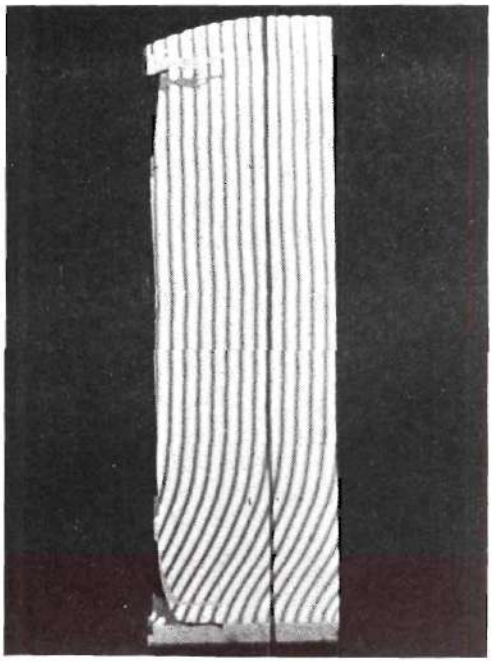

Figure 9. Sample Interferogram - Group One
Substance: Butyl Formate

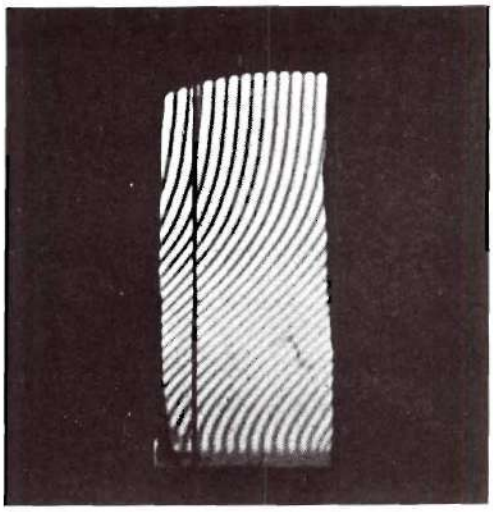

Figure 10. Sample Interferogram - Group Two
Substance: Methyl Acetate

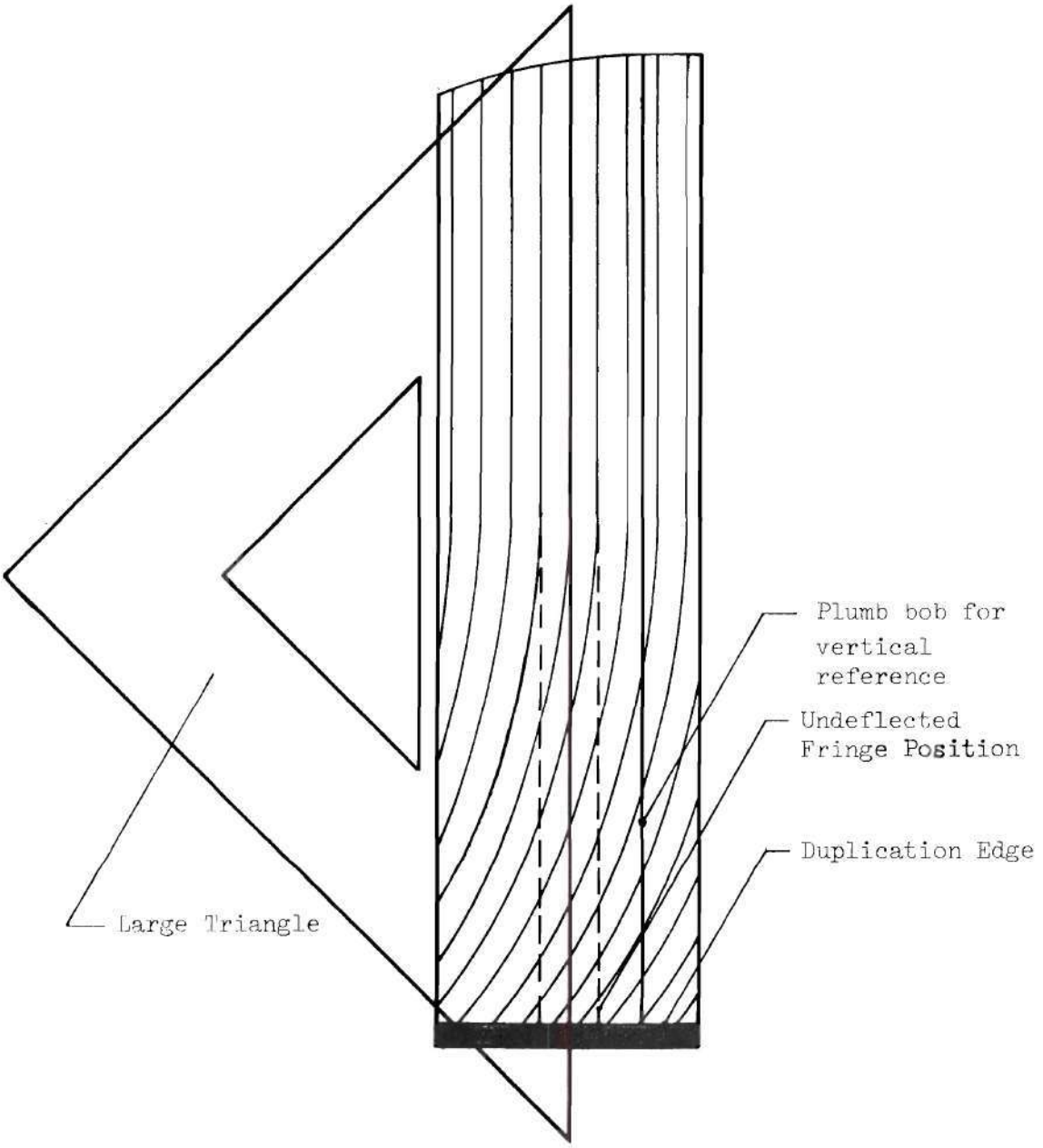

Figure 11. Determination of Undeflected Fringe Positions

was determined by counting the integer fringe shift and adding a fractional fringe shift determined by linear interpolation.

In the other tests this method for determining the undeflected positions could not be used since the new cell position allowed less of the fringes to be viewed. As the presence of the diffusing vapor spread up the cell, the length of the fringe that remained undeflected during the test was too short to accurately align the triangle. As a result, another measurement technique was developed for the tests in which the cell was higher in the interferometric field of view.

At the beginning of each test the camera was started before pulling the shim from the cell. The portion of the film containing the undeflected fringe pattern was used to produce a reference pattern. The plumb bob and center three fringes were traced on a large sheet of paper. This reference fringe pattern was then aligned using the plumb bob and short undeflected portion of the fringes at the top of the projected interferogram under analysis. A new reference pattern was produced in the above manner for each test.

After the undeflected fringe positions had been established, the deflections of the center three fringes were determined at the top of the duplication edge and at a line parallel to and 25.4 mm above it.

After the deflections of all the selected interferograms were read, the number of timing indicators between the analyzed frames were counted and entered on data reduction forms. A conversion factor of 0.00966 (derived from the timing pulse calibration) was applied to the number of indicators to convert to real time elapsed between data points in seconds. The cumulative time, starting with $t = 0$ for the first

interferogram reduced, and the time increments between interferograms were then determined.

The three readings of fringe shift at each height (top of duplication edge and 25.4 mm higher) were then averaged to produce two mean fringe shifts for each interferogram. The z dimensions were determined by using the known separation distance and by relating the measured projected cell width and actual cell width of 25.4 mm. The corrected fringe shift at the top of the duplication edge was then evaluated using Equations (II-57), (II-58), and (II-59). The factor P_{tr} given by Equation (II-63), was computed over several intervals during the test, averaged, and used with the other parameters gathered from the sources given in Chapter III to determine the diffusivity from Equation (II-61).

CHAPTER VI

RESULTS

The presentation of results in this chapter will be in approximate chronological order. Generally, the performance of the test equipment was satisfactory except that premature diffusion of more volatile substances past the seals caused termination of the testing before studying all of the candidate materials. The results of the tests do, however, allow conclusions to be drawn concerning the suitability of the differential interferometer in the determination of diffusivity. The testing was divided into several phases determined chiefly by the availability of the test equipment.

The first tests were performed without using the interferometer to establish techniques for working with the test cell. These tests produced several modifications in the design of the cell. It was found that the shim covering the liquid would be wetted when the cell was subjected to even slight vibration. The shim was elevated using spacers until the wetting ceased when the shim had been raised approximately 0.6 mm above the liquid surface. Other modifications were suggested including the relocation of thermocouples and improvements to the system of seals. Efficient assembly, disassembly, and cleaning techniques were also developed.

When the performance of the cell was thought to be satisfactory, it was placed on the stand in the interferometer for qualitative testing.

Grob [26] had experienced difficulty due to disruption of the fringe pattern caused by motion of the air adjacent to the shim as it was extracted. This potential problem was not encountered during the preliminary tests and did not occur during subsequent testing.

These early tests also demonstrated that the fringe patterns developed as predicted by theory. When the shim was removed, very large initial fringe deflection occurred near the surface with the number of fringe shifts diminishing rapidly with increasing distance from the surface. As time elapsed, the deflection of the fringes spread up the cell as the fringe shift at the interface decreased. Observation of the horizontal gradient indicated that only minimal departures from the one-dimensional assumption occurred in these preliminary tests.

The initial tests using the camera were made without a strip chart recorder. The lack of reliable interface temperature data rendered these tests qualitative since accurate measurements of that temperature was vital in determining the correct equilibrium mole fraction. Upon examination, the films of the first few tests showed a black area in the vicinity of the interface which obscured the fringes. The black area was observed at and immediately above the liquid surface as the shim was removed and it persisted several seconds into the test before gradually fading enough for the fringes to be observed. As additional time passed, the black area disappeared altogether. It is thought that the black area was the product of severe scatter of the light in the vicinity of the interface. Realignment of the interferometer and test cell reduced, but failed to eliminate, the black area

near the interface region.

After the realignment was completed, additional runs were made using samples of acetone. The tests with the best film clarity were selected for reduction to develop the data reduction method. In the reduction of one preliminary test, the deflection of the center fringe on nine interferograms spanning 3.6 seconds was measured. The interferograms were numbered with the frame nearest the start of the test designated number one. Since the reduction was to be qualitative due to the previously mentioned lack of interface temperature data, special attention was paid to the variation of parameter P of Equation (II-63) with time. Theoretically, P should be a constant throughout the test. The nine interferograms initially selected for reduction were at very short time intervals ($t_b - t_a$). Eight values of P were calculated from the nine interferograms and then averaged. The variation of individual values of P from the average was as high as ± 12.5 percent even though a plot of fringe shift versus time produced a seemingly smooth curve which was the expected behavior. Investigation of the variation of P showed that relatively small changes in the value of fringe shift caused relatively large changes in the value of P.

Checks on the reading error showed that for about ten fringe shifts, re-readings were usually within $\Delta m = 0.05$ of the original values. For fringe shifts of less than ten shifts the error was still about $\Delta m = 0.05$ which appeared to be the lower limit of the accuracy of the reading technique. Thus, an increasing percentage error could be encountered by attempting to read interferograms with less than ten fringe shifts. As a result, interferograms with less than ten fringe shifts were avoided

whenever possible. For the larger fringe shifts ($m > 20$), re-reading variations were as large as $\Delta m = 0.1$. This was due to the decreased film clarity and the much narrower, more sharply inclined fringes encountered near the start of the test. However, due to the very large number of fringe shifts, the larger Δm produced no more percentage error than the smaller Δm later in the test. Errors of the magnitude encountered in reading the fringe shift were capable of producing the large scatter in the computed values of P for the short time intervals being used.

It was found that the variation in P could be reduced by selecting the pairs of interferograms to be compared at longer time intervals. Thus, instead of comparing interferograms 1 and 2, 2 and 3, 3 and 4, etc., interferograms 1 and 5, 2 and 6, etc. were compared to find the value of P. (The interferograms were numbered consecutively starting with the frame closest in time to the time of shim removal.) In the case of the particular preliminary test under consideration, this new procedure reduced the variation in P to $\pm$ 5.0 percent. The new method was adopted for use in all future tests since it apparently produced a more accurate value of the test parameter P.

When a strip chart recorder became available, further preliminary tests were performed to determine the behavior of the system temperatures in the vicinity of the liquid-air interface. As expected the thermocouple at the liquid surface showed temperature depressions when the shim was removed. This confirmed the need to continuously monitor the interface temperature due to the desire to have an accurate determination of the vapor pressure of the diffusing substance. The output of the

thermocouple immedaitely above the interface was also being monitored and consistently indicated an increase on the order of 0.5°K in temperature when the diffusion process was started. Since a decrease in temperature had been expected, additional tests were made to determine the reason for this behavior. Variations in diffusing substance, location of thermocouples, recording equipment, and room conditions changed only the magnitude of the temperature increase. No tests except those in which liquid acetone was purposely applied to the thermocouple bead with the cell disassembled produced temperature decreases. A possible explanation of this phenomenon could involve the adsorption of the diffusing vapor on the thermocouple bead which would produce the indicated temperature increase.

The temperature recorded by the near-air thermocouple that exhibited the unexpected increase in temperature was used to calculate the air properties and to check for thermal equilibrium before starting each test. Since the molar refractivity of air is a weak function of the temperature and the increase recorded was of a small magnitude, the behavior of the thermocouple was not considered to adversely effect the results of the tests.

The tests discussed to this point were made using the three degree Wollaston prism sensitivity setting. No significant fringe deflection was detected in the air above the shim before the shim was removed. Fringe deflections prior to shim removal would have indicated premature vapor leakage past the shim. Leakage of the test liquids from the cell occurred on approximately one-half of the attempted tests indicating the need for a refined cell charging procedure.

The preliminary tests were considered encouraging enough to proceed with the determination of the method accuracy by measuring the diffusivities of the reference materials. Tests of toluene, methanol, n-hexane, methyl propionate, methyl acetate, butyl formate, and butyl bromide were filmed. The first five of these substances have well documented diffusivities and were to be used as reference substances. The tests on toluene, methanol, methyl propionate and butyl formate from the above list were reduced.

Observations of the film for data reduction indicated that only the tests made using the eight degree Wollaston prisms were suitable for analysis due to the appearance of the black area described previously. The tests using the lower sensitivity setting (one and three degree prisms), had the critical interface region blacked out over such a long time interval that the number of fringe shifts fell below the desired lower limit of ten by the time the black area had disappeared. Since the eight degree prisms produced proportionally greater fringe deflection at a given time, sufficiently large number of fringe shifts could be observed by the time the black area had disappeared. It was, therefore, decided that all future tests would be conducted using the higher sensitivity setting. This allowed for sufficient fringe deflections to be measured to minimize reading errors. Also, the recording of fringe shifts at long times from the instant of shim removal should have permitted the effects of initial transients within the system to have been minimized.

Since longer test intervals result from the use of higher interferometer sensitivity settings, the possible breakdown of the infinite

tube assumption must be considered. Evaluation of Equation (II-21) using nominal diffusivities and vapor pressures showed that the boundary condition of zero concentration of diffusing vapor at the top of the test cell was not violated. For the most volatile of the tested substances, the time required for diffusing particles to reach the top of the cell was approximately three times the duration of the tests.

After another realignment of the test cell-interferometer system was made (using a new technique), a second series of tests was run. This group consisted of tests on acetone, methyl acetate (re-run), ethyl formate, vinyl acetate, butyl bromide (re-run) and dibromomethane. The films of most of the tests in this group showed extreme horizontal variations across the cell caused by sloshing of the test liquids. The realignment allowed viewing of this phenomenon for the first time in which the crests of waves could be seen moving rapidly back and forth across the cell. Of the eleven test films in this group only the tests of acetone, vinyl acetate, dibromomethane and methyl acetate were reduced. The remaining films were of very poor quality. More than one-half of the tests attempted in this group were not filmed because of leakage of the test liquid from the cell before the shim could be removed. This leakage was due to the rapid deterioration of the seals in the ends of the channel caused by the exposure to the test liquids.

The test substances used in the second group of tests generally were of greater volatility than those previously tested and were thus capable of producing greater fringe deflections. This fact, combined with the use of the higher sensitivity setting of the interferometer allowed the observation of leakage of vapor past the covering shim.

The films showed that the initial condition of pure air above the shim was not being met in nearly all of the tests. Deflections of up to one-half fringe existed at the shim before starting some tests. Efforts to remove residual vapor with compressed air proved futile as the diffusing vapor was leaking past the shim at too great a rate.

Based on poor simulation of the initial condition for substances tested in the second group and the even higher volatilities of the remaining candidate substances, the conclusion was reached that the cell was not capable of producing accurate, repeatable results for the higher volatility substances. Therefore, the taking of data was abandoned. Data on the reference substances is presented to demonstrate the increasing error produced by cell leakage with increasing volatility.

Table 1 shows the values of the diffusivity of the reference substances compared with the values obtained by other investigators. It can be seen that the method of this study produces consistently lower values of the diffusivity than those measured by other investigators. The test values have been corrected to a 25°C, 760 mm Hg condition using Equation (V-1).

$$D_{AB_{25°C,\ 760\ mm\ Hg}} = D_{AB_{T,P}} \left(\frac{298}{T} \right)^2 \left(\frac{P}{760} \right) \qquad (V\text{-}1)$$

where P is in mm of mercury and T in degrees Kelvin. The best results are seen to be for the lower volatility substances while the error generally increases with increasing vapor pressure.

Although the exponent in Equation (V-1) is known to vary, the second power best represents the substances under consideration [26, 39,

72]. Since the tests were carried out at temperatures between 22°C and 25°C, the impact of the temperature correction is small and is not a factor in the discrepancy between tested and reference values of the diffusivity.

Diffusivities of previously untested substances determined in this study and corrected to 25°C and 760 mm Hg are given below:

$D_{\text{Butyl Formate-Air}} = 0.0940 \text{ cm}^2/\text{sec}$

$D_{\text{Vinyl Acetate-Air}} = 0.0697 \text{ cm}^2/\text{sec}$

$D_{\text{Dibromomethane-Air}} = 0.0552 \text{ cm}^2/\text{sec}$

Caution must be exercised in the use of these values since no better accuracy may be expected than in the case of the reference substances. Thus, the reported diffusivity values are quite probably lower than the true diffusivities.

Table 1. Reference Substance Test Results

All D_{AB} Corrected to T = 25°C & P = 760 mm Hg

Units of cm^2/sec

Substance	D_{AB} This Study	% Low	D_{AB} Average of Other Investigators	References	P_v [mm Hg] @ 25°C
Toluene	0.813	3.9%	0.0846	[39],[51],[72]	29
Methanol	0.150	4.5%	0.157	[39],[51],[72]	120
Methyl Acetate	0.0757	23.5%	0.0989	[39],[72]	208
Methyl Propionate	0.0829	4.6%	0.0869	[39],[72]	84
Acetone	0.0928	13.3%	0.1070	[39],[52]	229

Note: None of the tests made with additional reference substances n-hexane and ethyl formate were of sufficient quality for reduction.

CHAPTER VII

CONCLUSIONS

A method has been developed for measurement of the mass diffusivity of volatile liquids. The method utilizes fringe shift data produced by a differential interferometer applied to a transient one-dimensional evaporation model. The method was used to determine the mass diffusivity of eight substances; five reference substances with well documented values of mass diffusivity and three unknown substances whose diffusivity has previously been unreported. The accuracy of the method decreased as the substance volatility increased. Values for the low volatility substances were within 4 percent of published values while those for the higher volatility materials differed by as much as 24 percent.

The chief cause of inaccuracy in this study was the poor simulation of the theoretical model by the cell; specifically, violation of the initial condition. Leakage of vapor past the covering shim caused contamination of the air above the shim before starting each test. The presence of the diffusing substance in significant quantity above the shim caused gradients smaller than predicted by theory to be measured early in the test. The gradients detected later in each test were closer to the theoretical values. The deviation from the theoretical rate of change of gradient test parameter P_{tr} which in turn resulted in low diffusivity values. The leakage past the shim also diminished

the repeatability that the system should have demonstrated since different amounts of leakage occurred in each test.

It is apparent that a high degree of accuracy was not attainable with the current cell. The liquid must be completely isolated from the stagnant air before the test is started. This necessitates seals for the ends of the shim making viewing of the surface impossible. However, since the simplification obtained by surface viewing ($z = 0$ implies $E = 0$) proved illusory, the inability to view the interface should not incapacitate future investigations. Problems will arise in fringe deflection measurement away from the interface due to difficulties in obtaining accurate positional data. A referencing system could overcome this problem, allowing accurate determination of distance from the interface. Another problem will arise due to the rapid decrease in fringe shift with distance from the interface which is particularly noticable in the early stages of each test. Since potential error increases with decreasing fringe shift, the distance from the interface in which accurate measurements may be made is limited.

While it is possible for the differential interferometer and cell used in this study to produce reasonably accurate diffusivity data for low volatility substances the disadvantages of the method must be considered.

1. The number of substances that may be interferometrically investigated is limited. Many materials do not have the combination of volatility and molar refractivity necessary for production of sufficient fringe deflections for accurate measurement. The need for both optical

and physical data and the requirement of moderate toxicity further limit the number of candidates.

2. It is the nature of the equations to amplify errors in measurement of the fringe shift and vapor pressure.

3. Adaptation of the system to measure diffusivity at temperatures and pressures other than those in the laboratory would be very difficult.

Although the method of diffusivity measurement developed in this study might be refined to produce more accurate data, the physical difficulties encountered outweigh the advantages gained by use of the technique. The conclusion must be drawn that other means of diffusivity measurement are capable of producing more accurate experimental values with the expenditure of less time and effort.

BIBLIOGRAPHY

1. Adams, J. A. and Meier, L. B., "Density Gradients Near a Liquid/Air Interface," Report NRL-6828, (AD 686 659), Naval Research Laboratory, Washington, D. C., March 31, 1969.

2. Antwiler, H. J., "Method of Measurement for Sedimentation, Electrophoresis, and Diffusion Phenomena, Using an Apparatus with a Great Light Transmitting Capacity. An Instrument for the Measurement of Diffusion Constants," Chemie-Ingenieur - Technik, Vol. 24, pp. 284-288, May 1952.

3. Arnold, J. H., "Studies in Diffusion: III. Unsteady-State Vaporization and Absorption," American Institute of Chemical Engineers Transactions, Vol. 40, pp. 361-377, 1944.

4. Bierlein, J. A., "Gouy Diffractometry in Thermal Diffusion," Journal of Chemical Physics, Vol. 36, No. 10, pp. 2793-2802, May 15, 1962.

5. Bird, R. B., Stewart, W. E. and Lightfoot, E. N., Transport Phenomena, John Wiley and Sons, Inc., New York, c. 1960.

6. Black, W. Z. and Carr, W. W., "Application of a Differential Interferometer to the Measurement of Heat Transfer Coefficients," The Review of Scientific Instruments, Vol. 42, pp. 337-340, 1971.

7. Black, W. Z. and Carr, W. W., "A Differential Interferometer and its Application to Heat and Mass Transfer Measurements," ASME Paper No. 72-HT-12, presented at the ASME-AICHE Heat Transfer Conference, Denver, Colorado, August, 1972.

8. Boyd, C. A., Stein, N., Steingrimsson, V., and Rumpel, W. F., "An Interferometric Method for Determining Diffusion Coefficients in Gaseous Systems," Journal of Chemical Physics, Vol. 19, No. 5, pp. 548-553, May 1951.

9. Bryngdahl, O., "A New Interferometric Method for the Determination of Diffusion Coefficients of Very Dilute Solutions," Acta Chemica Scandinavica, Vol. 11, No. 6, pp. 1017-1033, 1957.

10. Bryngdahl, O., "Interferometric Studies of Boundary Formations and Deviations from Ideality in Diffusion Experiments," Acta Chemica Scandinavica, Vol. 12, pp. 684-700, 1958.

11. Bryngdahl, O. and Ljunggren, S., "New Refractive Index Gradient Recording Interferometer Suitable for Studying Diffusion, Electro-

phoresis and Sedimentation," Journal of Physical Chemistry, Vol. 64, No. 9, pp. 1264-1270, September 1960.

12. Bryngdahl, O. and Ljunggren, S., "New Calculation Methods and Requirements of the Shear Interferometric Determination of Diffusion Coefficients," Acta Chemica Scandinavica, Vol. 16, pp. 2162-2176, 1962.

13. Bryngdahl, O., "Wavefront Shearing Interferometer for Direct Recording of Refractive Index Gradient in Cartesian Coordinates," Journal of the Optical Society of America, Vol. 53, No. 5, pp. 571-576, May 1963.

14. Caldwell, C. S., Hall, J. R., and Babb, A. L., "Mach-Zehnder Interferometer for Diffusion Measurements in Volatile Liquid Systems," Review of Scientific Instruments, Vol. 28, No. 10, pp. 816-821, October 1957.

15. Carr, W. W., "The Measurement of Instantaneous, Local Heat Transfer from a Horizontally Vibrating Isothermal Cylinder Using a Differential Interferometer," Doctor of Philosophy Thesis, Georgia Institute of Technology, 1973.

16. Chanu, J., Mousselin, L. and Parra, F., "Interferometric Method for Measurement of Weak Variations in the Index Gradient of Liquids," Revue d'Optique, Vol. 41, No. 3, pp. 119-130, March 1962.

17. Coulson, C. A., Cox, J. T., Ogston, A. G., and Philpot, J. St. L., "A Rapid Method for Determining Diffusion Coefficients in Solution," Proceedings of the Royal Society, A, Vol. 192, pp. 382-402, February 18, 1948.

18. Crank, J. and Robinson, C., "Interferometric Studies in Diffusion, II. Influence of Concentration and Orientation on Diffusion in Cellulose Acetate," Proceedings of the Royal Society, A, Vol. 204, pp. 549-569, January 9, 1951.

19. Dreisbach, R. R., Pressure-Volume-Temperature Relationships of Organic Compounds, 3rd Edition, Handbook Publishers, Inc., Sandusky, Ohio, c. 1952.

20. Dreisbach, R. R., Physical Properties of Chemical Substances, Dow Chemical Company, Midland, Michigan, 1953.

21. Duda, J. L., Sigelko, W. L., and Vreitas, J. S., "Binary Diffusion Studies with a Wedge Interferometer," Journal of Physical Chemistry, Vol. 73, No. 1, pp. 141-149, 1969.

22. El-Wakil, M. M. and Jaeck, C. L., "A Two Wavelength Interferometer for the Study of Heat and Mass Transfer," Journal of Heat Transfer,

Vol. 86, No. 3, pp. 464-466, 1964.

23. El-Wakil, M. M., Myers, G. E., Schilling, R. J., "An Interferometric Study of Mass Transfer from Vertical Plate at Low Reynolds Number," Journal of Heat Transfer, Vol. 88, No. 4, pp. 399-406, November 1966.

24. Emmert, R. E. and Pigford, R. L., "A Study of Gas Absorption in Falling Liquid Films," Chemical Engineering Progress, Vol. 50, No. 2, pp. 87-93, 1954.

25. Gleason, M. N., Editor, Clinical Toxicology of Commercial Products, 3rd Edition, Williams and Wilkins Company, Baltimore, Maryland, c. 1969.

26. Grob, A. K., "An Interferometric Technique for Measuring Binary Diffusion Coefficients," Doctor of Philosophy Thesis, University of Wisconsin, 1967.

27. Grob, A. K. and El-Wakil, M. M., "An Interferometric Technique for Measuring Binary Diffusion Coefficients," Journal of Heat Transfer, Vol. 91, No. 2, pp. 259-266, 1969.

28. Haluska, J. L., Colver, C. P., "Diffusion Coefficients for the System Toluene/Methyl-cyclohexane by Using Birefringence Interferometry," AICHE Journal, Vol. 16, No. 4, pp. 691-693, July 1970.

29. Hariharan, P. and Sen, D., "Three Beam Interferometer for Diffusion Measurements," Journal of Scientific Instruments, Vol. 39, No. 4, pp. 165-167, April 1962.

30. Hawley, G. G., Editor, Condensed Chemical Dictionary, 8th Edition, Van Nostrand-Reinhold Company, New York, N. Y., c. 1971.

31. Hook, L., Davis, W. W., Kotin, L., "High Speed Calculation of Diffusion Coefficients from Rayleigh Interference Fringes," Applied Optics, Vol. 2., No. 1, pp. 66-77, January 1963.

32. Ingelstam, E., "Measurements of Optical Path Gradients by Means of Birefringence Interferences. Liquid Gradients, in Particular, Determination of Diffusion Constants," Arkiv for Fysik, Vol. 9, Paper 12, pp. 213-226, 1955.

33. Inoue, Y., Osugi, A., Inoue, T., "Improvement of the Diffusion Cell for Measurement of Diffusion Coefficient by the Schlieren Knife Edge Method," Kagaku Kogaku, Vol. 29, No. 8, pp. 628-629, 1965.

34. Jordan, E. T., Vapor Pressures of Organic Compounds, Interscience Publishers, Inc., New York, N. Y., c. 1954.

35. Kegeles, G. and Gostling, L. J., "The Theory of an Interference Method for the Study of Diffusion," Journal of the American Chemical Society, Vol. 69, pp. 2516-2523, October 1947.

36. Longsworth, L. G., "Experimental Tests of an Interference Method for the Study of Diffusion," Journal of the American Chemical Society, Vol. 69, pp. 2510-2516, October 1947.

37. Longsworth, L. G., "Tests of Flowing Junction Diffusion Cells with Interference Methods," Review of Scientific Instruments, Vol. 21, pp. 524-528, June 1950.

38. Loschmidt, J., Akad. Wiss. Wien., Vol. 62, p. 468, 1870.

39. Lugg, G. A., "Diffusion Coefficients of Some Organic and Other Vapors in Air," Analytical Chemistry, Vol. 40, No. 7, pp. 1072-1077, June 1968.

40. McCabe, W. L. and Smith, J. C., Unit Operations of Chemical Engineering, McGraw-Hill Book Company, Inc., New York, N. Y., c. 1956.

41. Mellan, I., Ketones, Chemical Publishing, New York, New York, c. 1968.

42. Monick, J. A., Alcohols, Their Chemistry, Properties and Manufacture, Reinhold Book Corporation, New York, N. Y., c. 1968.

43. Nicolas, L. and Calvet, E., "Improvements in the Interferometer Method for Recording Vertical Diffusion and Sedimentation in Liquids," Comptes Rendus Hebdomadaires Des Seances De L Acadamie Des Sciences, Vol. 228, pp. 559-561, February 14, 1949.

44. Nishijima, Y. and Oster, G., "Moiré Patterns: Their Application to Refractive Index and Refractive Index Gradient Measurements," Journal of the Optical Society of America, Vol. 54, No. 1, pp. 1-5, January 1964.

45. Ogston, A. G., "The Gouy Diffusiometer; Further Calibration," Proceedings of the Royal Society, A., Vol. 196, pp. 272-285, March 1949.

46. Paul, D. R., "Measurement of Diffusion Coefficients for Concentrated Binary Polymer Solutions," Industrial and Engineering Chemistry Fundamentals, Vol. 6, No. 2, pp. 217-222, May 1967.

47. Perry, R. H., Editor, Chemical Engineers Handbook, McGraw-Hill Book Company, Inc., New York, N. Y., c. 1963.

48. Philpot, J. St. L. and Cook, G. H., "A Self Plotting Interferometric Optical System for the Ultracentrifuge," Research London, Vol. 1, pp. 234-236, February 1948.

49. Porsch, B. and Kubin, M., "Limits of Use of a Polarization Interferometer for the Measurement of Diffusion Coefficients at Very Low Concentrations," Collection of Czechoslovak Chemical Communications, Vol. 33, No. 4, pp. 1028-1037, 1968.

50. Prasad, C., Chen, C. S., Beard, J. T., "An Interferometric Technique for Temperature and Concentration Measurement for an Air-Water Interface," Journal of Basic Engineering, Paper No. 70-WA/Temp-1, August, 1970.

51. Reid, R. C. and Sherwood, T. K., The Properties of Gases and Liquids, McGraw-Hill Book Company, Inc., New York, N. Y., c. 1958.

52. Richardson, J. F., "The Evaporation of Two-Component Liquid Mixtures," Chemical Engineering Science, Vol. 10, pp. 234-242, 1959.

53. Robinson, C., "Interferometric Studies in Diffusion, I. Determination of Concentration Distributions," Proceedings of the Royal Society, A., Vol. 204, pp. 339-359, December 22, 1950.

54. Ross, P. A. and El-Wakil, M. M., "Two Wavelength Interferometric Technique for the Study of Vaporization and Combustion of Fuels," Progress in Astronautics and Rocketry, Vol. 2, pp. 265-298, 1960.

55. Sadovnikov, G. V., Smol'skiy, B. M., and Shchitnikov, V. K., "Investigation of Simultaneous Heat and Mass Transfer Using an Interferometer," Heat Transfer, Soviet Research, Vol. 1, No. 1, 1969.

56. Saini, G. and Moraglio, G., "A Micrometric Method for Determining the Coefficients of Diffusion in Solutions," Annali D. Chimica, Vol. 42, pp. 239-246, 1952.

57. Schrader, W., Differential Interferometer, WSW Fine Instruments and Optics, Wenden, Germany, April 1960.

58. Stephan, J., Wien Ber. II, Vol. 68, p. 385, 1873.

59. Stoll, D. R., "Vapor Pressure of Pure Substances," Industrial and Engineering Chemistry, Vol. 39, No. 4, pp. 517-550, April 1947.

60. Svensson, H., "An Interferometric Method for Reading the Refractive Index Derivative in Concentration Gradients," Acta Chemica Scandinavica, Vol. 3, pp. 1170-1178, 1949.

61. Svensson, H., "An Optical Arrangement for Getting Simultaneous Records of the Refractive Index and its Derivative for Stratified Solutions," Acta Chemica Scandinavica, Vol. 4, pp. 399-403, 1950.

62. Svensson, H., "An Interferometric Method for Recording the Refractive Index Derivative in Concentration Gradients, II.

Arrangement for and the Theory of the Purely Optical Differentiation of the Refractive Index Function," Acta Chemica Scandinavica, Vol. 4, pp. 1329-1346, 1950.

63. Svensson, H., "On the Use of Rayleigh-Philpot-Cook Interference Fringes for the Measurement of Diffusion Coefficients," Acta Chemica Scandinavica, Vol. 5, pp. 72-84, 1951.

64. Svensson, H., "Production of High Intersity, Multifringe, Rayleigh Interference Patterns," Acta Chemica Scandinavica, Vol. 5, pp. 1301-1310, 1951.

65. Svensson, H., "On the Use of Rayleigh-Calvet-Philpot Interference Fringes for the Measurement of Diffusion Coefficients According to the Moment Method," Acta Chemica Scandinavica, Vol. 5, pp. 1410-1412, 1951.

66. Svensson, H. and Odengrim, K., "A New Method of Measuring Small Refractive Index Differences," Acta Chemica Scandinavica, Vol. 6, pp. 720-728, 1952.

67. Thomas, W. J. and Nicholli, E. McK., "The Application of the Wave-front Shearing Optical Interferometer to Diffusion Measurements," Applied Optics, Vol. 14, No. 7, pp. 823-829, July 1965.

68. Touloukian, Y. S., Editor, Thermophysical Properties Research Literature Retrieval Guide, 2nd Edition, Plenum Press, New York, N. Y., c. 1967.

69. Travnicek, E. A. and Fan, L. T., "A Modified Microinterferometric Technique for Measurement of Diffusion Coefficients of Liquids," Review of Scientific Instruments, Vol. 40, No. 7, pp. 930-935, July 1969.

70. Tung, L. N. and Drickamer, H. G., "Diffusion Through an Interface-Binary System," Journal of Chemical Physics, Vol. 20, pp. 6-12, 1952.

71. Wallin, L. E., "Thermal Diffusion Measurements with a Modified Savart Interferometer," Journal of Chemical Physics, Vol. 52, No. 2, pp. 552-556, January 15, 1970.

72. Washborn, E. W., Editor, International Critical Tables of Numerical Data, Physics, Chemistry and Technology, McGraw-Hill Book Company, Inc., New York, N. Y., c. 1926.

73. Watkins, L. S. and Tvarusko, A., "Lloyd Mirror Laser Interferometer for Diffusion Studies," Review of Scientific Instruments, Vol. 41, No. 2, pp. 1860-1866, 1970.

74. Weast, R. C., Editor, Handbook of Chemistry and Physics, 51st Edition, Chemical Rubber Company, Cleveland, Ohio, 1970-1971.

75. Weinstein, W., "An Interferometer for Simultaneous Observation of Concentration and Concentration Gradient in Liquid Columns," Nature, Vol. 172, pp. 461-462, September 5, 1953.

REFERENCES NOT CITED

1. Altshuller, A. P. and Cohen, I. R., "Application of Diffusion Cells to the Production of Known Concentrations of Gaseous Hydrocarbons," Analytical Chemistry, Vol. 32, No. 7, pp. 802-810, June 1960.

2. Chen, N. H. and Othmer, D. F., "New Generalized Equation for Gas Diffusion Coefficient," Journal of Chemical and Engineering Data, Vol. 7, No. 1, pp. 37-41, January 1962.

3. Fan, L. T. and Tseng, J. T., "Apparent Diffusivity in Honey-Water System," Journal of Food Science, Vol. 32, pp. 633-636, 1967.

4. Fuller, E. N., Schettler, P. D., Giddings, J. C., "A New Method for Prediction of Binary Gas-Phase Diffusion Coefficients," Industrial and Engineering Chemistry, Vol. 58, No. 5, pp. 19-27, May 1966.

5. Ibrahim, S. H. and Kuloor, N. R., "Diffusion in Binary Gas System," British Chemical Engineering, Vol. 6, No. 12, pp. 862-863, December 1961.

6. Lee, C. Y. and Wilke, C. R., "Measurements of Vapor Diffusion Coefficient," Industrial and Engineering Chemistry, Vol. 46, No. 11, pp. 2381-2387, November 1954.

7. Roberts, J., "Estimation of Binary Diffusion Coefficients for Air-Polar and Air-Non-Polar Gas Systems," British Chemical Engineering, Vol. 8, No. 11, pp. 753-757, November 1963.

8. Strehlow, R. A., "The Temperature Dependence of the Mutual Diffusion Coefficient for Four Gaseous Systems," Journal of Chemical Physics, Vol. 21, No. 12, pp. 2101-2106, December 1953.

9. Valasek, J., Introduction to Theoretical and Experimental Optics, John Wiley and Sons, Inc., New York, N. Y., c. 1949.

10. Welty, J. R., Wicks, C. E. and Wilson, R. E., Fundamentals of Momentum, Heat and Mass Transfer, John Wiley and Sons, Inc., New York, N. Y., c. 1969.